Electronic Supplementary Material (ESI) for Chemical Science.

Supplementary Information

Spontaneous emergence of membrane-forming protoamphiphiles from a lipid-amino acid mixture under wet-dry cycles

Manesh Prakash Joshi[1], Anupam A. Sawant[1], and Sudha Rajamani[1*]

[1]Department of Biology, Indian Institute of Science Education and Research, Pune 411008, India.

[*]Corresponding Author:
Dr. Sudha Rajamani
Department of Biology
Indian Institute of Science Education and Research,
2nd Floor, Main Building, Dr. Homi Bhabha Road,
Pune, Maharashtra-411008 (INDIA).
Phone (O): +91- 020- 25908061
Fax (O): +91- 020- 25899790
srajamani@iiserpune.ac.in

Materials and Methods

Materials. All the phospholipids and NAA standards were purchased from Avanti polar lipids (USA). The rest of the chemicals and reagents, including amino acids, were bought from Sigma-Aldrich (India). All reagents were of analytical grade and used without further purification.

Setting up the reaction. In a typical reaction, adequate volume of 25 mg/ml POPC chloroform stock, required to prepare 200 µl of 8 mM POPC solution, was taken in a glass vial. The chloroform was evaporated to form a dry lipid film, which was rehydrated with 200 µl of 80 mM Gly pH 9.8 solution to get a mixture of the Gly and the POPC in 10:1 ratio. This solution was then subjected to wet-dry cycles at 90°C on a heating block (RCT basic, IKA). Each wet-dry cycle duration was 24 hours, where a solution was allowed to evaporate to dryness at 90°C and again rehydrated after 24 hours with 200 µl of nanopure water, and vortexed briefly to remix the components. The same procedure was followed for multiple wet-dry cycles. At the end of wet-dry cycling, the reaction was rehydrated with 200 µl of nanopure water, vortexed and stored at 4°C until further analysis. Other reactions like only Gly (80 mM) and only POPC (8 mM) control reactions, and those with other amino acids and phospholipids, were also performed under the same reaction conditions, excepting for a few variations in some reactions. In POPC concentration variation experiments, the concentration of Gly was maintained at 80 mM while that of POPC was varied as 4 mM, 8 mM and 16 mM to get Gly to POPC ratios of 20:1, 10:1 and 5:1, respectively. In the Lys + POPC reaction, pH was set to 9.1 in order to account for the lower pka of α-amino group of Lys (8.9). In the Asp + POPC reaction, 30 mM Asp and 3 mM POPC (10:1 ratio) was used due to the low solubility of Asp in water. In the Gly + POPC reaction under acidic conditions, the pH was 3.

Separation of lipids from Gly oligomers in a reaction mixture. Before mass analysis, lipids were separated from Gly oligomers using the butanol-hexane extraction. Briefly, 100 µl of the reaction mixture was diluted by adding 200 µl of nanopure water. To this diluted sample, 300 µl of butanol was added and vortexed briefly. The solution was then centrifuged at 13,000 rpm for 1 minute. The upper butanol layer was collected in a separate vial and the butanol extraction step was repeated once again. Then, 150 µl of hexane was added to the aqueous layer. This solution was vortexed and centrifuged at 13,000 rpm for 1 minute. The upper hexane layer was removed carefully and the remaining solution was evaporated to dryness at 30°C in CentriVap DNA vacuum concentrator (Labconco). The dry layer was dissolved in 100 µl of nanopure water to reconstitute the aqueous phase containing free Gly and its oligomers, which was analysed by LC-MS. Whereas, the butanol phase containing all the lipids was separately collected and analysed using HRMS. For experiments involving the quantification of Gly oligomers, a control reaction containing 80 mM Gly without POPC was also subjected to BH extraction to account for the loss of Gly oligomers during the extraction process.

Detection and quantification of Gly oligomers. Gly oligomers formed in the Gly control and the Gly + POPC reactions were analysed by LC-MS (ExionLC coupled with X500R-QTOF MS; SCIEX). Samples were prepared from the aqueous phase of the BH extraction mixture, with 1:10 dilution in nanopure water and acidified with 0.1% v/v formic acid, to which 10 nmoles of dialanine was added as an internal standard. Samples were injected in 50 µl aliquots into a reversed phase C_{18} column (Phenomenex Luna 5 µm C18(2) 100 Å, 250×4.6 mm) attached to a guard column (Phenomenex Luna 5 µm C18(2) 100 Å, 50×4.6 mm), which were eluted at 0.5 ml/min flow rate with a linear gradient mixture of solvents A (water + 0.1% v/v formic acid) and B (100% acetonitrile

+ 0.1% v/v formic acid) over 32 minutes as follows: 0 min, 100% A; 4 min, 100% A; 14 min,35% B; 15 min, 100% B; 23 min, 100% B; 24 min, 100% A; 32 min, 100% A.

For the TOFMS and MS/MS analysis, following parameters were used: ion source temperature = 400°C, ion polarity was positive, ionspray voltage = 5500 V, declustering potential = 70 V, collision energy (CE) was 5 eV for MS analysis and a collision energy spread of 20 eV was used during MS/MS analysis to induce optimum fragmentation. The identity of Gly oligomers was confirmed by checking for the expected oligomer mass in MS spectra, and their respective fragmentation patterns upon MS/MS analysis. Data acquisition and analysis was done using SCIEX OS software. The peak area of the internal standard (dialanine) was used to normalize the peak areas of Gly oligomers, which were then summed up to get the overall oligomer yield. All quantitation experiments were performed in at least 3 to 4 replicates, while the rest of the experiments were repeated independently at least two times.

Detection and identification of NAAs using TLC and HRMS. The Gly + POPC and other control reactions were analysed by TLC using a normal phase silica plate (Merck) using chloroform, methanol, and water (65:25:4) as a solvent system, and visualized by staining with either iodine or primuline. During the BH extraction of Gly + POPC and other control reactions, the butanol phase containing all the lipidic species in the reaction was collected separately. The butanol was then evaporated under vacuum, and the dry lipid film was re-suspended into methanol and analysed by HRMS (SYNAPT G2 High Definition Mass Spectrometer equipped with QTOF mass analyzer; Waters) through direct injection of the samples. Molecules were ionized using electrospray ionization (ESI) method in negative ion mode with capillary voltage of 3 kV. Sometimes positive ion mode was also used for the detection of POPC and its degradation products. The NAAs corresponding to other amino acids and phospholipids were also analysed similarly. For getting highly accurate mass data ($\leq$ 5 ppm), LockMass correction was applied using Leucine encephalin as an internal standard. The ppm error was calculated using the following formula:

$$\text{ppm error} = ((\text{observed mass} - \text{theoretical mass}) \div \text{theoretical mass}) * 1000000$$

The MS/MS analysis of NOG and NPG standards and reaction products was performed similarly in negative ion mode using a collision energy of 10 eV to induce fragmentation. Data acquisition and analysis was done using MassLynx software from Waters.

NMR analysis of NAA standards and reaction products. NMR samples were prepared by drying the butanol phases that were collected separately during the BH extraction of Gly + POPC (10:1) and 8 mM POPC control reactions. The dry lipid film was then dissolved in 750 µl of DMSO-d6. For NOG and NPG standards, 1 mg of the dry powder of the corresponding NAA was directly dissolved in 600 µl of DMSO-d6. All these samples were subjected to ^{1}H NMR analysis on a Bruker 400 MHz Spectrometer at IISER Pune NMR facility, and the corresponding NMR spectra were analysed using Mnova software from Mestrelab.

Vesicle formation by NAAs. In a typical reaction, an appropriate volume of NOG methanol stock (10 mg/ml) was taken in a microfuge tube. The methanol was evaporated under vacuum to form a dry lipid film, which was rehydrated with 100 µl of 200 mM buffer of appropriate pH to get a 6 mM final concentration of NOG. For NOS, a similar procedure was followed except that the stock solution (1 mg/ml) was prepared by dissolving a dry powder of NOS in a chloroform:methanol (8:2; v/v) solution, followed by gentle heating and sonication. For getting solutions of different pH

values, following buffers were used: sodium phosphate for pH 3, acetate for pH 4 and 5, MES for pH 6, HEPES for pH 7, bicine for pH 8 and 9, and CHES for pH 10. The reaction tubes were then incubated at 60°C on a thermomixer (eppendorf ThermoMixer C) for 1 hour with constant shaking at 500 rpm and immediately subjected to microscopy (Axio Imager Z1, Carl Zeiss) and visualized under 40X objective (NA = 0.75) using DIC and also with fluorescence microscopy. For fluorescence imaging, vesicles were stained with 10 µM amphiphilic dye called Octadecyl Rhodamine B Chloride (R18) (Invitrogen), which was generously shared by the Pucadyil lab at IISER Pune. Vesicle staining was achieved using appropriate volume of R18 dye in methanol stock, which was added while making the dry lipid film of NAAs. Fluorescent vesicles were visualized using filter set 43 HE (Ex: 550/25 nm, Em: 605/70 nm, Beamsplitter: FT 570). Image acquisition and video recording was done using AxioVision software.

Calcein encapsulation within NAA vesicles: A dry lipid film of NAA was hydrated with appropriate buffer (200 mM acetate pH 4 for NOS and pH 5 for NOG) containing 0.1 mM calcein, which is known to get spontaneously encapsulated during vesicle formation process. After the encapsulation of calcein, the vesicle solution was diluted 1:2 times with the same buffer but without calcein to reduce background fluorescence. Rest of the procedure for vesicle preparation and microscopic analysis is as described above, except for the one change wherein the fluorescence imaging was done using filter set 65 HE (Ex: 475/30 nm, Em: 550/100 nm, Beamsplitter: FT 495).

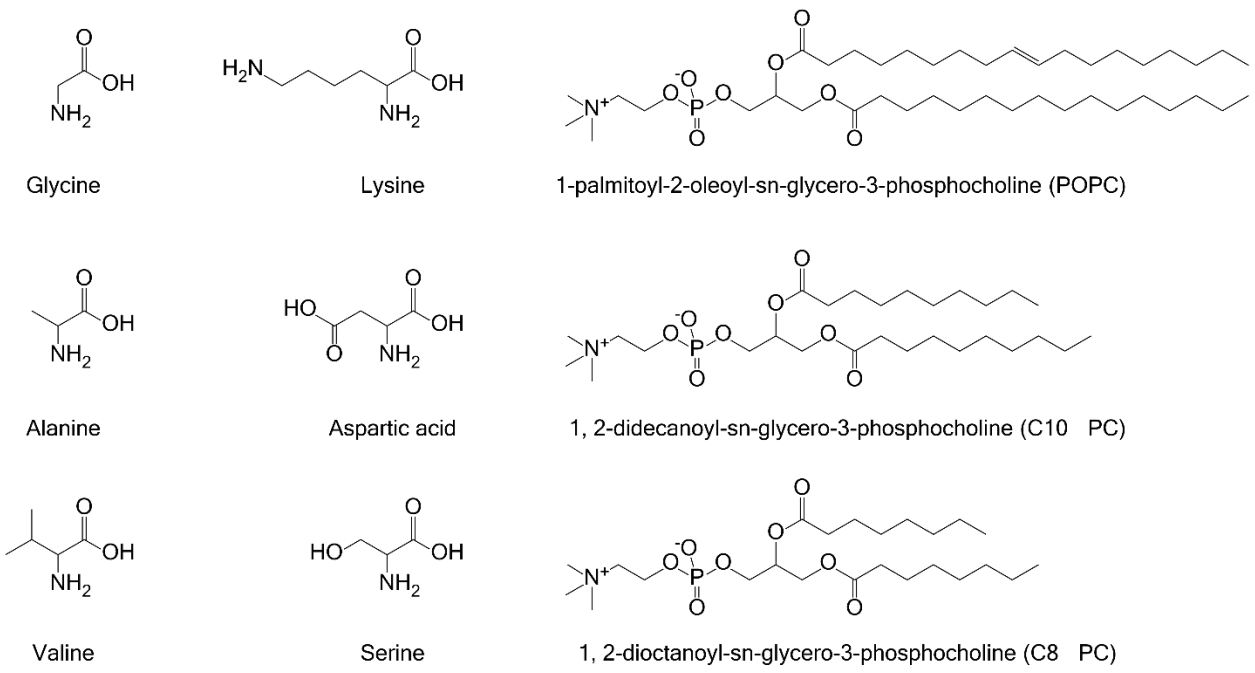

Figure S1 Different amino acids and phospholipids used in the study.

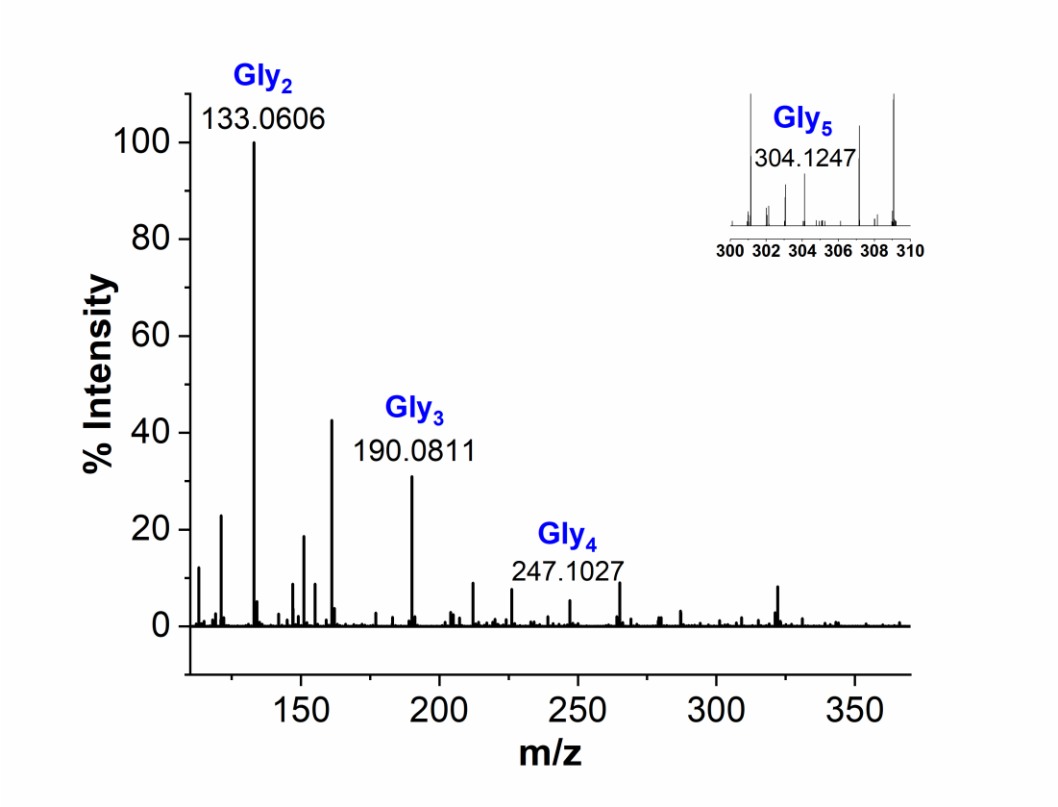

Figure S2 LC-MS analysis of different Gly oligomers formed in the presence of POPC under wet-dry cycles. Gly oligomers up to 6-mers were detected. However, the intensity of Gly_6 is too low to be observed in the spectrum.

Table S1 Masses corresponding to different Gly Oligomers that were detected during the LC-MS analysis of Gly control and Gly + POPC reactions.

Gly oligomer	Exact mass	Theoretical mass	Gly - POPC reaction		Gly + POPC reaction	
			Observed mass	Error	Observed mass	Error
		$[M+H]^+$	$[M+H]^+$	(ppm)	$[M+H]^+$	(ppm)
Gly_2	132.0535	133.0608	133.0607	-0.8	133.0606	-1.5
Gly_3	189.075	190.0822	190.0812	-5.3	190.0811	-5.8
Gly_4	246.0964	247.1037	247.1029	-3.2	247.1027	-4.0
Gly_5	303.1179	304.1252	304.1249	-1.0	304.1247	-1.6
Gly_6	360.1393	361.1466	361.1461	-1.4	361.1478	3.3

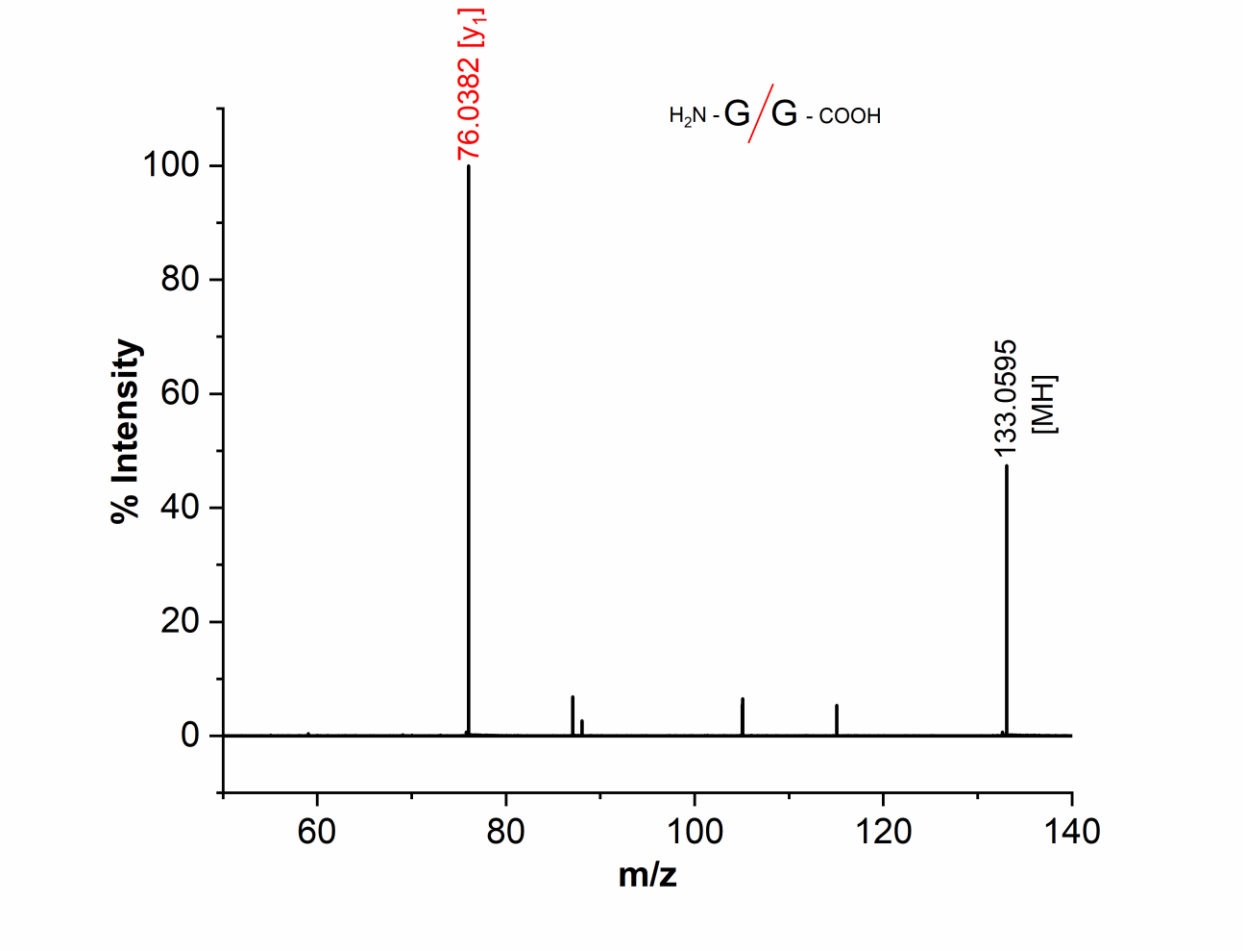

Figure S3 MS/MS analysis of diglycine (Gly_2) formed in the wet-dry cycling reaction. Expected masses corresponding to the precursor ion (diglycine; [MH]) as well as the y_1 ion are observed. Experimental data matches with the predicted fragmentation pattern of GG sequence. CE used was 16.7 eV.

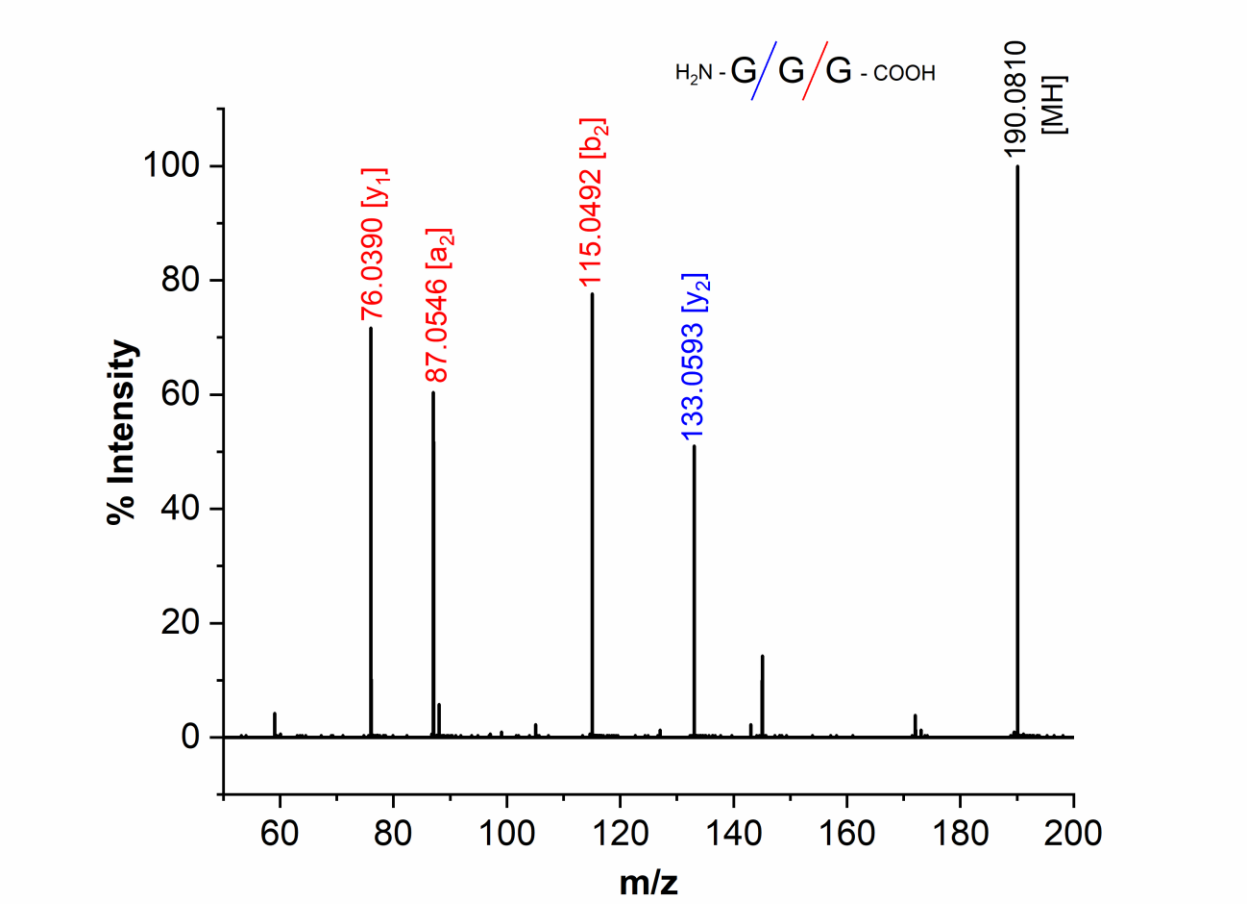

Figure S4 MS/MS analysis of triglycine (Gly_3) formed in the wet-dry cycling reaction**.** Expected masses corresponding to the precursor ion (triglycine; [MH]) as well as y, b, and a types of ions are detected. Experimental data matches with the predicted fragmentation pattern of GGG sequence. CE used was 19.9 eV. As peptide linkage is most susceptible to breakage during peptide fragmentation among the different backbone bonds, it leads to the generation of N-terminal b type ion and C-terminal y type ion. a type ions, which often form by the loss of CO from b type ion, are also frequently seen. A colored '/' symbol in the figure indicates the position of the peptide bond breakage in the sequence, and the corresponding y, b, and a type ions that are generated due to this breakage are also shown using the same color. Number in the subscript indicates the number of residues present in the ion. The MS/MS spectra for the Gly oligomers in the subsequent supplementary figures should also be interpreted in the same way as described here.

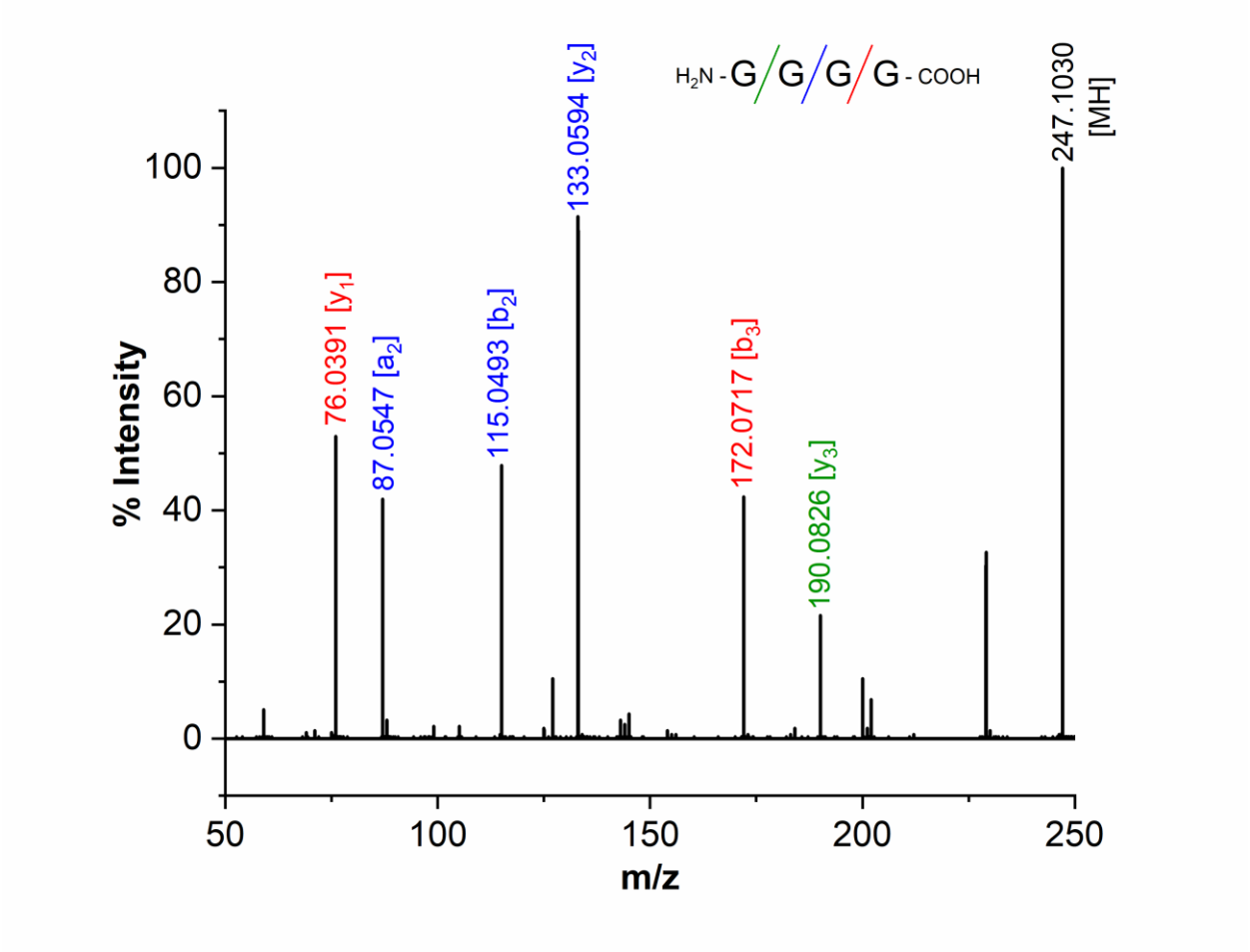

Figure S5 MS/MS analysis of tetraglycine (Gly_4) formed in the wet-dry cycling reaction. Expected masses corresponding to the precursor ion (tetraglycine; [MH]) as well as the most commonly observed y, b, and a fragments generated during peptide fragmentation, are detected. Experimental data matches with the predicted fragmentation pattern of GGGG sequence. CE used was 23.2 eV.

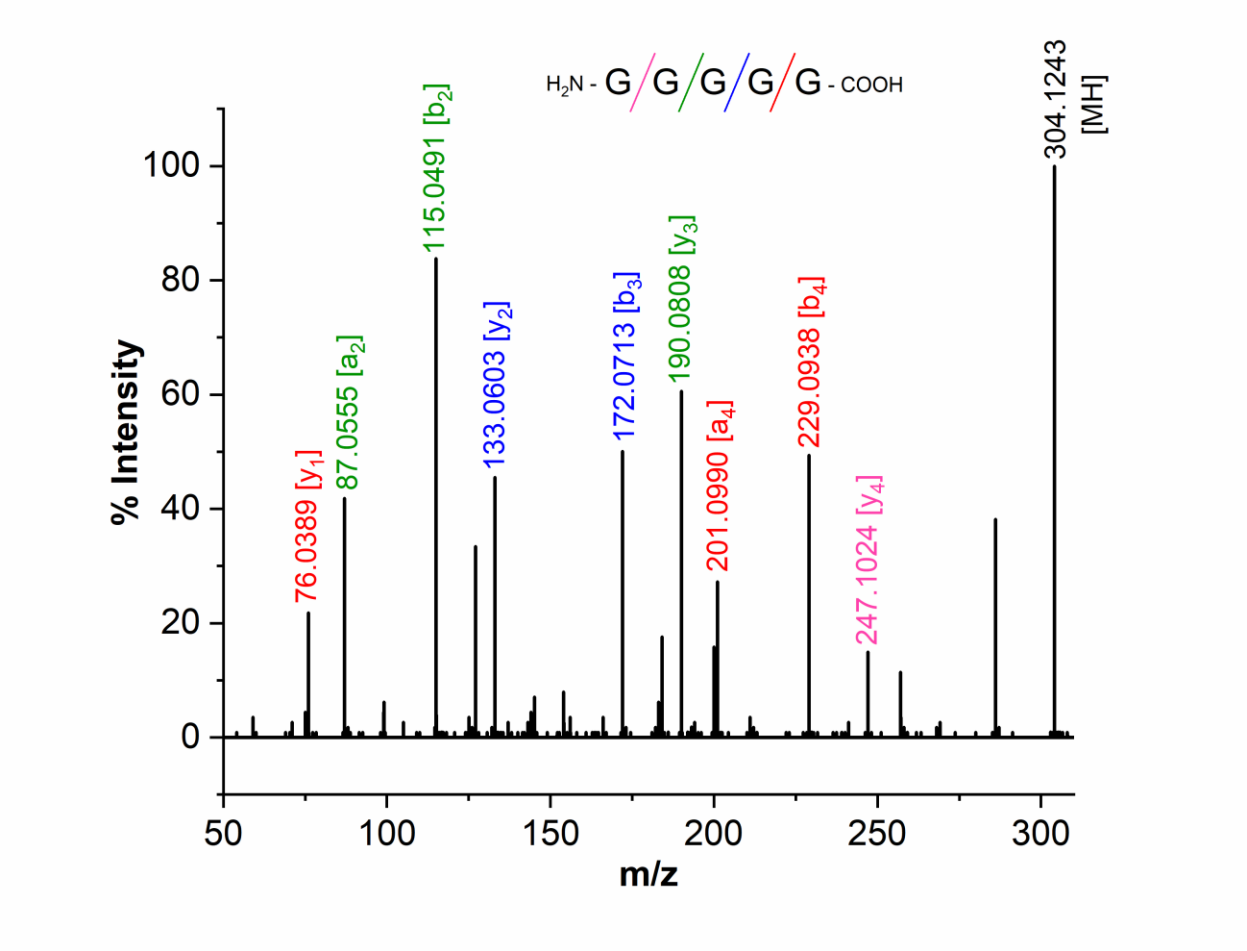

Figure S6 MS/MS analysis of pentaglycine (Gly_5) observed in the wet-dry cycling reaction. Expected masses corresponding to the precursor ion (pentaglycine; [MH]) as well as the most commonly observed y, b, and a fragments generated during peptide fragmentation, were detected. Experimental data matches with the predicted fragmentation pattern of GGGGG sequence. CE used was 26.5 eV.

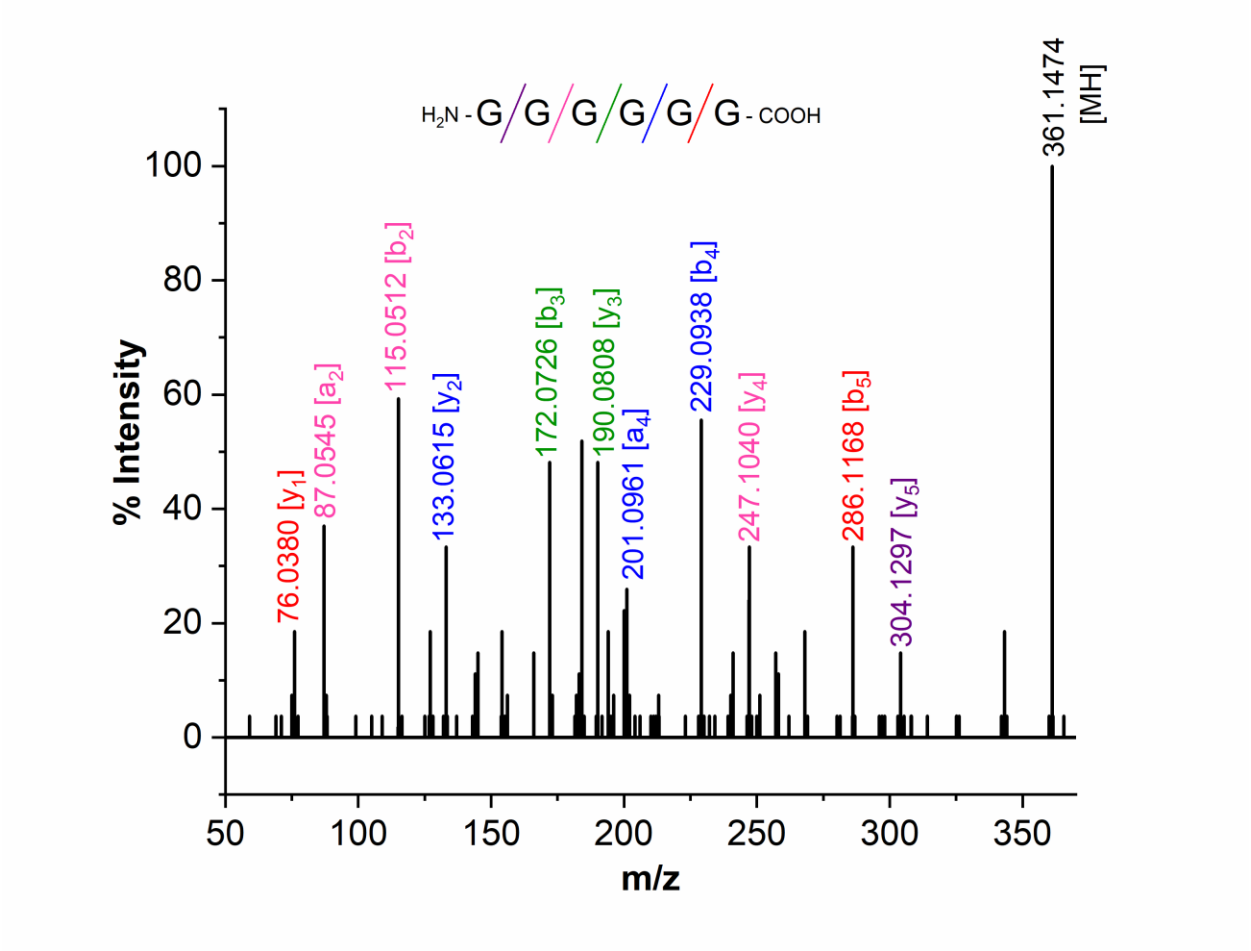

Figure S7 MS/MS analysis of hexaglycine (Gly_6) observed in the wet-dry cycling reaction. Expected masses corresponding to the precursor ion (hexaglycine; [MH]) as well as the most commonly observed y, b, and a fragments, are detected. Experimental data matches with the predicted fragmentation pattern of GGGGGG sequence. CE used was 29.8 eV.

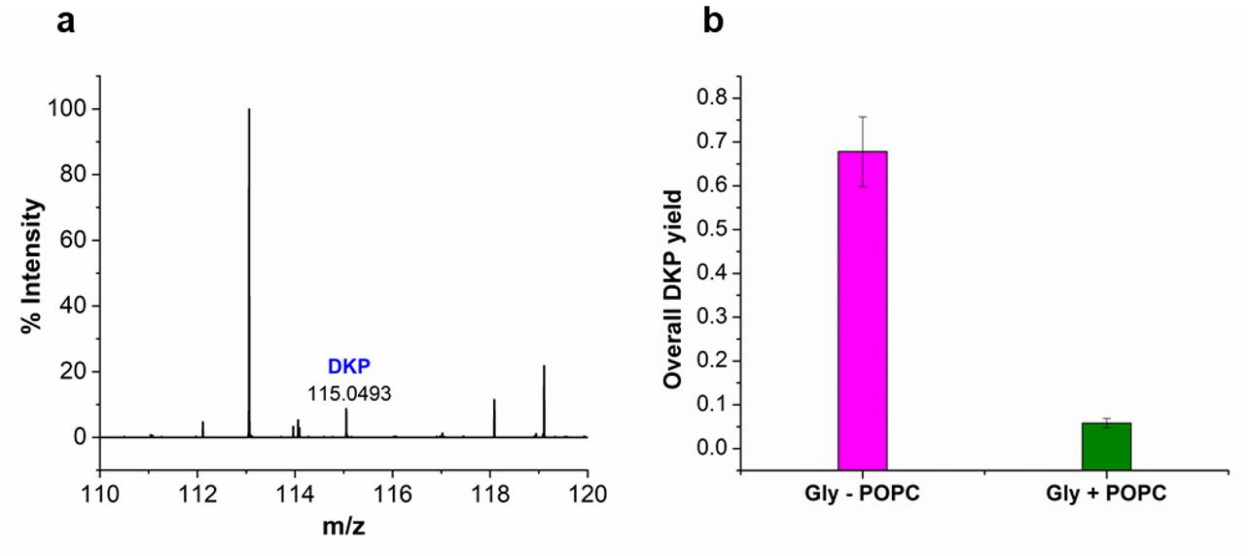

Figure S8 Formation of DKP under wet-dry cycles and the effect of POPC on its yield. (**a**) Diketopiperazine (DKP), a cyclic dipeptide of Gly, is observed in the 80 mM Gly pH 9.8 reaction that underwent five wet-dry cycles at 90°C. (**b**) The overall yield of DKP is lower in the presence of 4 mM POPC. These results indicate that the presence of POPC has an overall similar effect on both the main reaction (linear peptide formation) as well as the side reaction (DKP formation) of the peptide synthesis process. The detection and quantitation of DKP formation was done by LC-MS in a positive mode. Error bars in **b** represent standard deviation (N = 4).

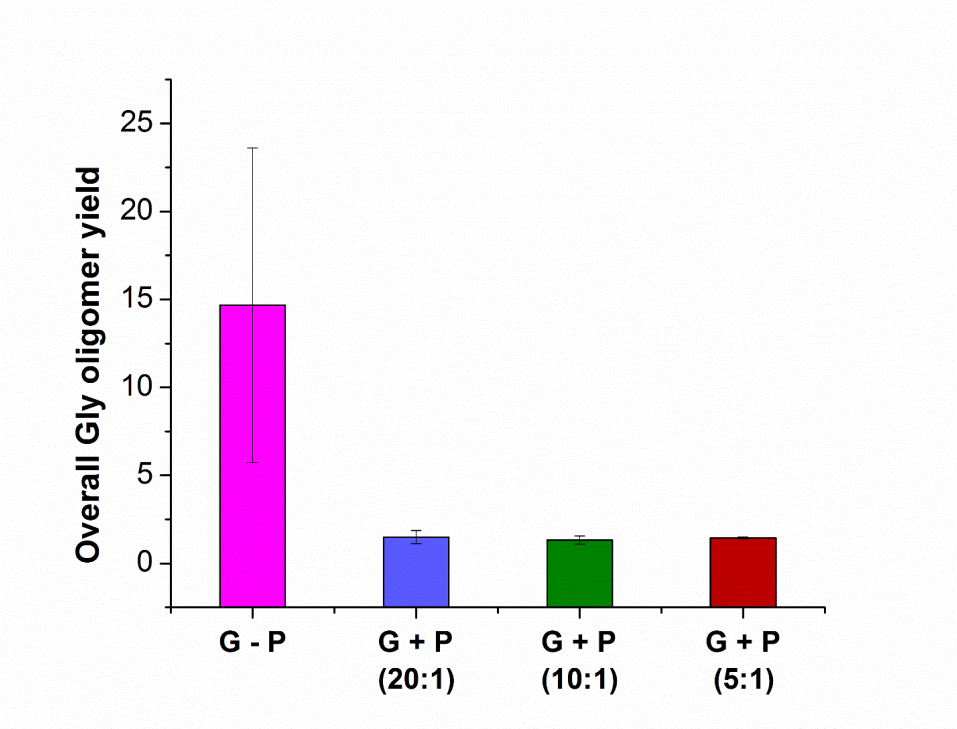

Figure S9 Effect of POPC on Gly oligomer yield with varying Gly to POPC ratios. The observed effect of POPC on Gly oligomer yield is consistent over different concentrations of POPC, where the overall yield decreases in the presence of POPC. The Gly concentration is 80 mM and the POPC concentration is varied as 4 mM (G + P; 20:1), 8 mM (G + P; 10:1), and 16 mM (G + P; 5:1), respectively. G – P represents the control reaction, which contains only Gly (80 mM). The overall yield was quantified using LC-MS in a positive ion mode. Error bars represent standard deviation (N = 3).

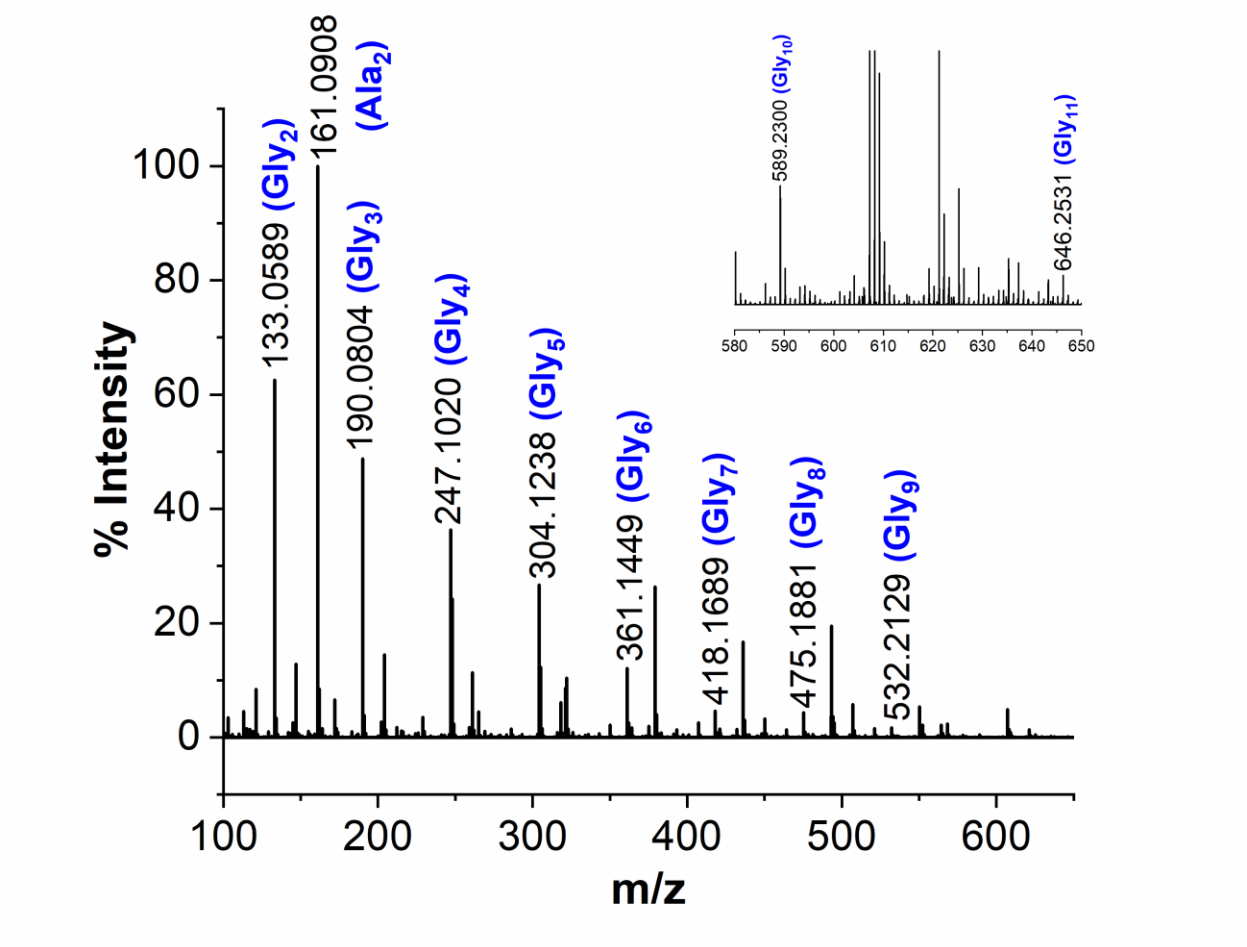

Figure S10 Formation of Gly oligomers under wet-dry cycle at 130°C. LC-MS analysis of 80 mM Gly reaction that underwent wet-dry cycling at 130°C, shows the formation of Gly oligomers up to 11-mers immediately after a single wet-dry cycle. The analysis was done in a positive ion mode. A mass corresponding to dialanine can also be observed in the spectrum, which was added as an internal standard during the analysis.

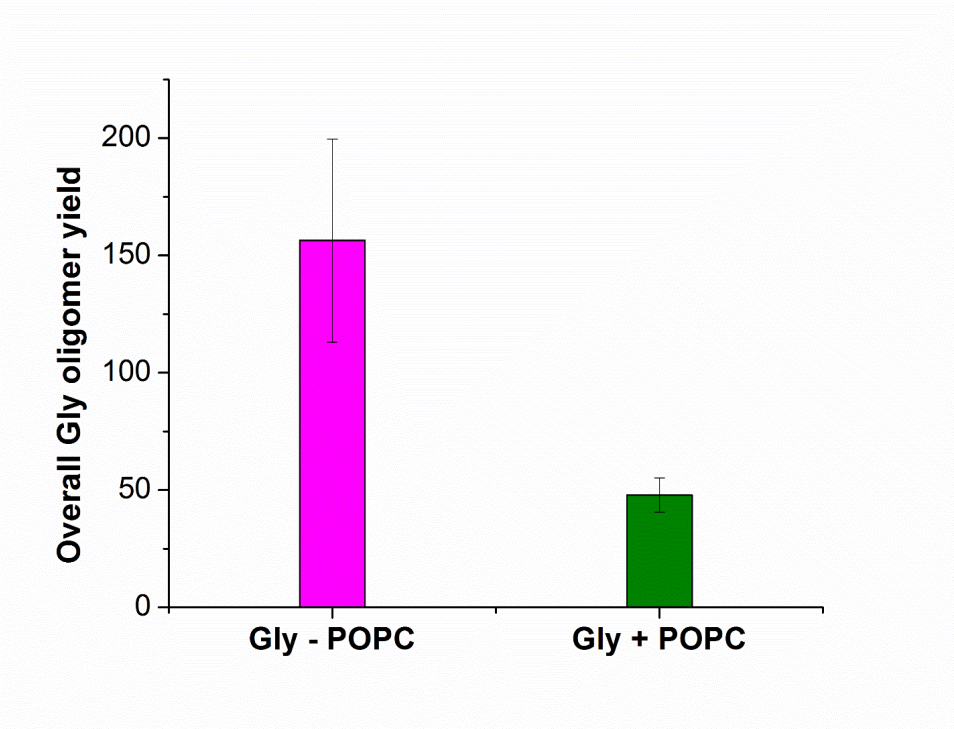

Figure S11 Effect of POPC on overall glycine oligomer yield at 130°C. Although, peptide synthesis occurs more readily at 130°C than 90°C, the effect of POPC on the overall oligomer yield is similar to that of the 90°C reaction, wherein the yield is lower in the presence of POPC (Gly + POPC) as compared to the control reaction (Gly – POPC). The concentrations of Gly and POPC are 80 mM and 4 mM respectively (Gly to POPC ratio is 20:1). Oligomers were quantified using LC-MS in a positive ion mode. Error bars represent standard deviation (N = 4).

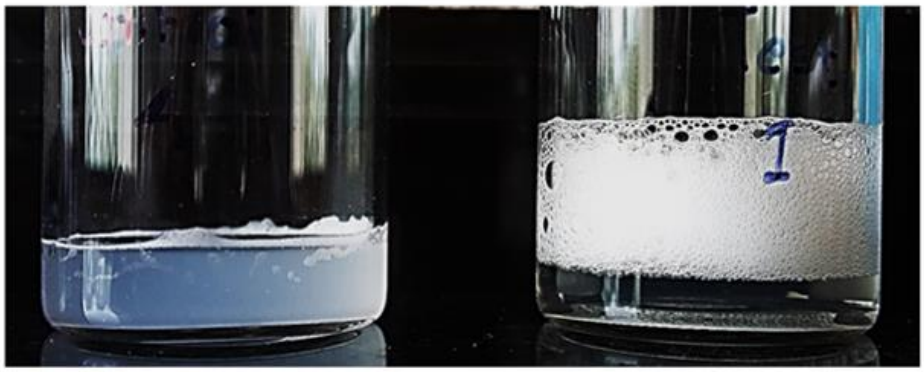

Figure S12 Conversion of POPC to the new product causes a change in the appearance of the reaction. After five wet-dry cycles at 90°C, the POPC control reaction (left) remains opalescent in nature, while Gly + POPC reaction (right) becomes transparent, with the accumulation of foam upon vortexing. However, to begin with both the solutions are opalescent.

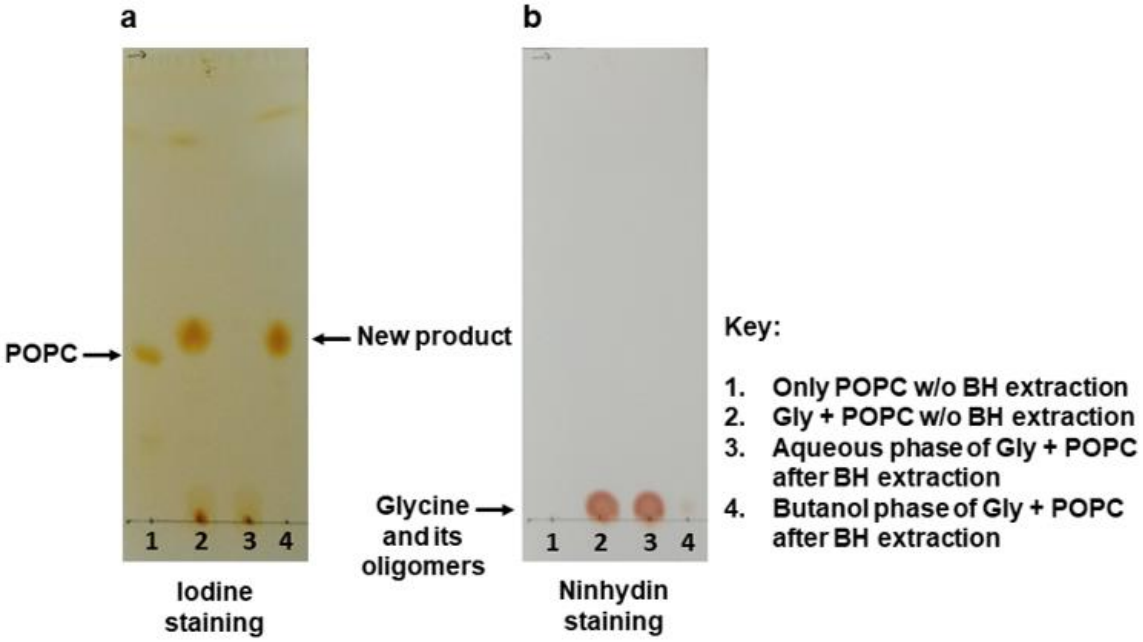

Figure S13 Insight into the plausible chemical nature of the new product. Preliminary TLC analysis shows that (**a**) the new product formed in the Gly + POPC reaction after wet-dry cycling (lane 2), preferentially goes into the butanol phase (lane 4), but not into the aqueous phase (lane 3) upon butanol-hexane extraction, suggesting its plausible lipidic nature. Bands were visualized with iodine staining. (**b**) The iodine was allowed to evaporate completely and the same TLC plate was subjected to ninhydrin staining, which shows that the new product cannot be stained by ninhydrin, indicating the absence of free amino group in it. The ninhydrin staining also confirmed that the Gly and its corresponding oligomers in the Gly + POPC reaction (lane 2), remain in the aqueous phase (lane 3) after the butanol-hexane extraction. The TLC analysis was performed on a normal phase silica plate using chloroform, methanol, and water (65:25:4) as a solvent system.

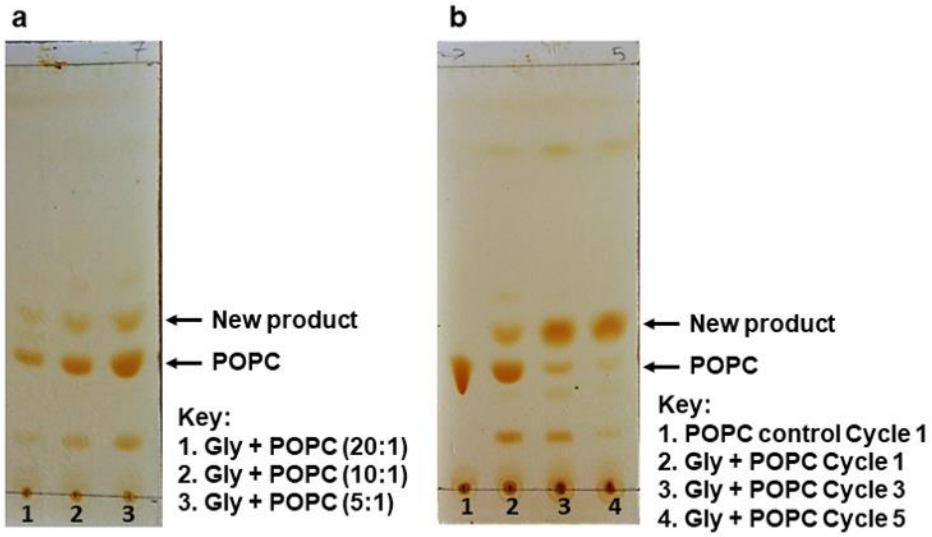

Figure S14 Effect of POPC concentration and wet-dry cycles on the formation of new product. (**a**) The intensity of the new band increases with increasing POPC concentration (lanes 1-3). The Gly concentration is 80 mM while the POPC concentration varies as 4 mM (Gly + POPC; 20:1), 8 mM (Gly + POPC; 10:1), and 16 mM (Gly + POPC; 5:1), respectively. (**b**) The conversion of POPC to the new product increases with increasing wet-dry cycles (lanes 2-4), and almost all of the POPC gets converted to the new product by the end of five wet-dry cycles (lane 4). There are few other bands observed in the Gly + POPC reaction (lanes 2 and 3), which are also present in the TLC in panel **a**. These bands possibly correspond to the transient species formed during the conversion of POPC to the new product, which almost disappear over five wet-dry cycles (lane 4). The TLC analysis was performed on a normal phase silica plate using chloroform, methanol, and water (65:25:4) as the solvent system, and the bands were visualized with iodine staining.

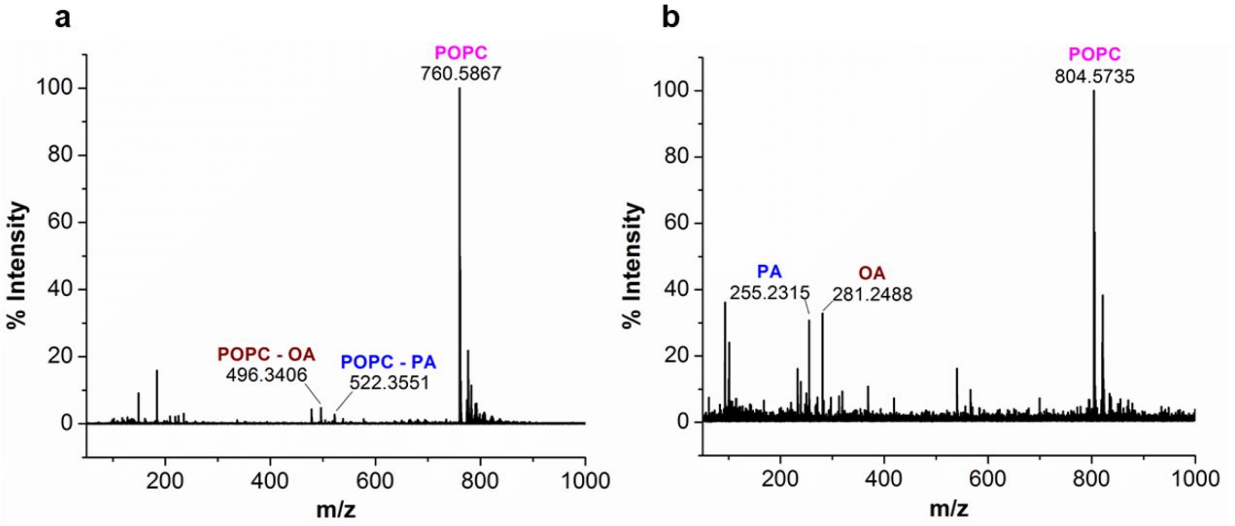

Figure S15 HRMS analysis of POPC control reaction. The HRMS analysis of the POPC only control reaction in (**a**) positive and (**b**) negative ion mode shows masses corresponding to POPC and its hydrolysis products, but not that of NPG and NOG. The hydrolysis products of POPC include free fatty acids like palmitic acid (PA) and oleic acid (OA) as observed in **b**, and also sn-glycero-3-phosphocholine attached to a single acyl chain, which is either palmitoyl group (POPC – OA), or oleoyl group (POPC – PA), as is observed in **a**. The reaction was subjected to five wet-dry cycles at 90°C and the concentration of POPC was 8 mM.

Table S2 Masses corresponding to different amphiphiles that were detected during the HRMS analysis of POPC control and Gly + POPC reactions.

Reaction	Chemical species	Exact mass	Ion type	Theoretical mass	Observed mass	Error (ppm)
Gly + POPC	NPG	313.2617	$[M-H]^-$	312.2544	312.2529	-4.8
	NOG	339.2773		338.2701	338.2697	-1.2
Only POPC	PA	256.2402	$[M-H]^-$	255.233	255.2315	-5.9
	OA	282.2559		281.2486	281.2488	0.7
	POPC	759.5778	$[M+HCOO]^-$	804.576	804.5735	-3.1
			$[M+H]^+$	760.5851	760.5867	2.1
	POPC – PA	521.3481	$[M+H]^+$	522.3554	522.3551	-0.6
	POPC – OA	495.3325		496.3398	496.3406	1.6

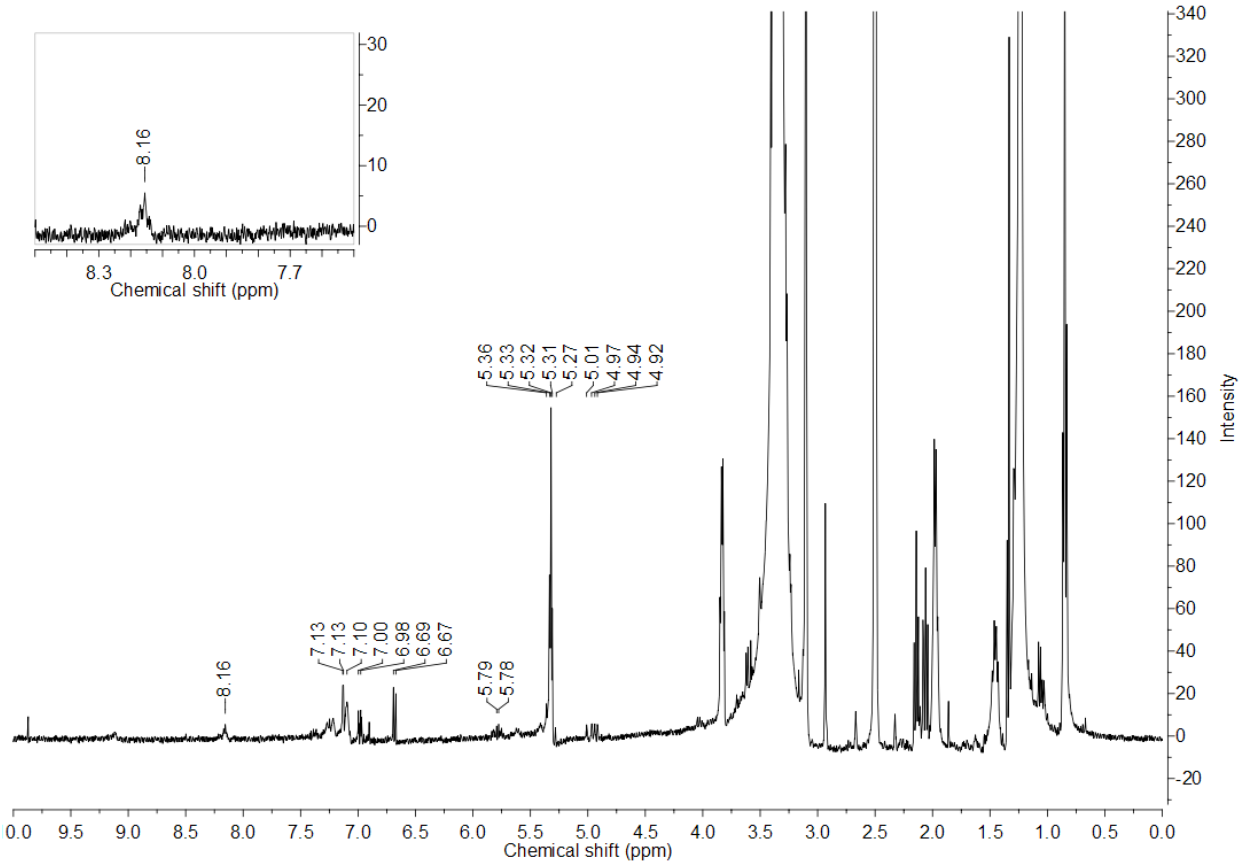

Figure S16 ^{1}H NMR analysis of Gly + POPC reaction**.** Full ^{1}H NMR spectrum of the butanol phase derived from the BH extraction of the Gly + POPC reaction that contains both NPG and NOG, along with other lipidic species that could arise either during the reaction between Gly and POPC, or due to the hydrolysis of POPC. A signature peak unique to both NPG and NOG is observed at 8.16 ppm (see inset), which comes from the exchangeable hydrogen attached to the nitrogen atom of the amide linkage present in NPG and NOG. The solvent used was DMSO-d6.

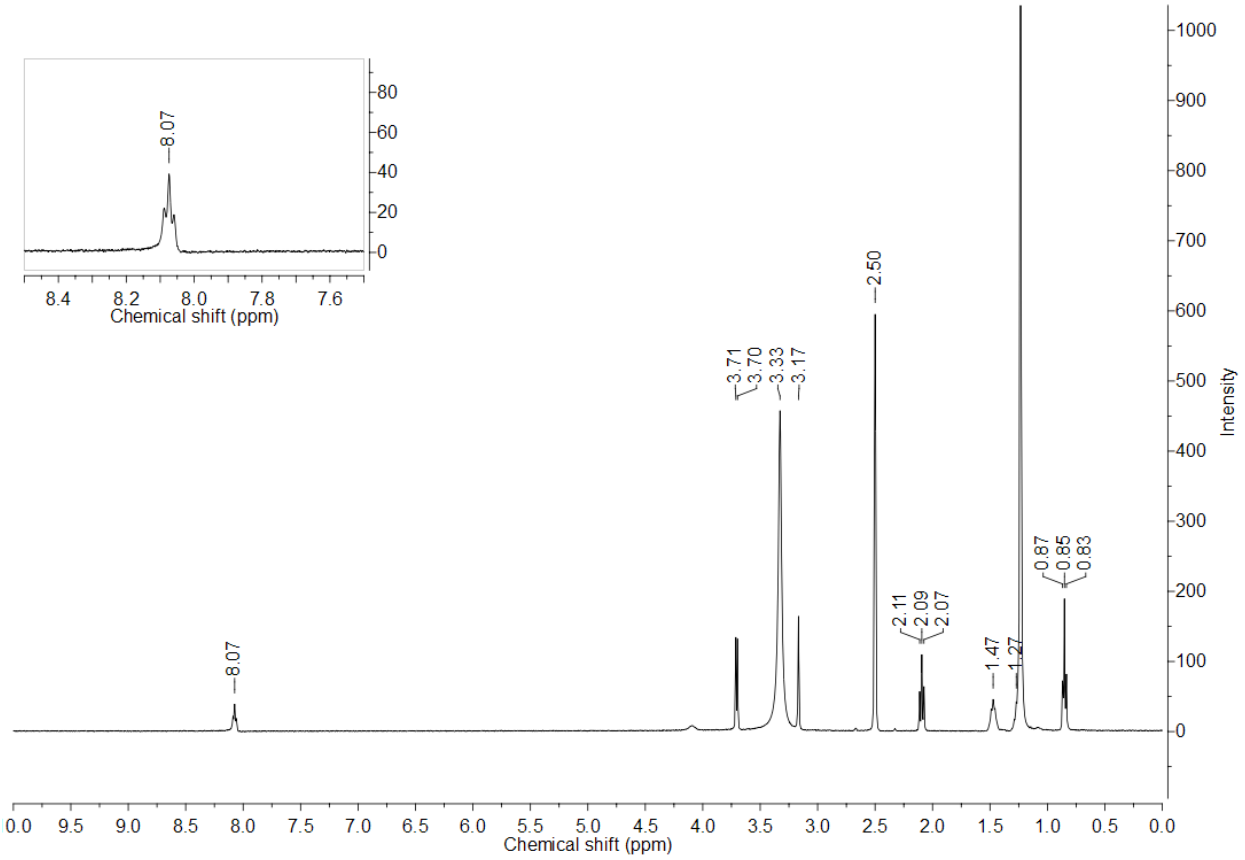

Figure S17 ^{1}H NMR analysis of the NPG standard. Full ^{1}H NMR spectrum of the commercially purchased NPG standard. A signature peak corresponding to the exchangeable hydrogen attached to the nitrogen atom of the amide linkage is observed at 8.07 ppm (see inset). The solvent used was DMSO-d6.

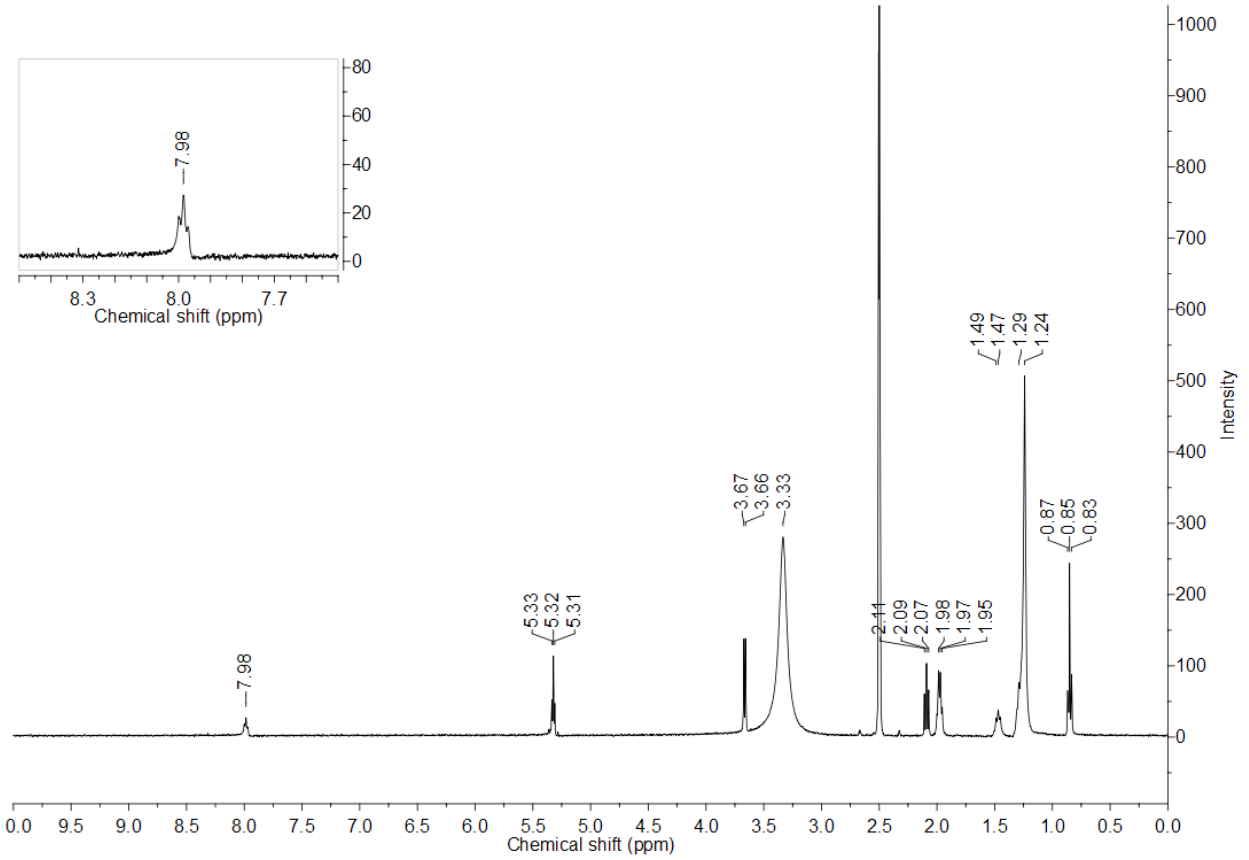

Figure S18 ^{1}H NMR analysis of the NOG standard. Full ^{1}H NMR spectrum of the commercially purchased NOG standard. A signature peak corresponding to the exchangeable hydrogen attached to the nitrogen atom of the amide linkage is observed at 7.98 ppm (see inset). The solvent used was DMSO-d6.

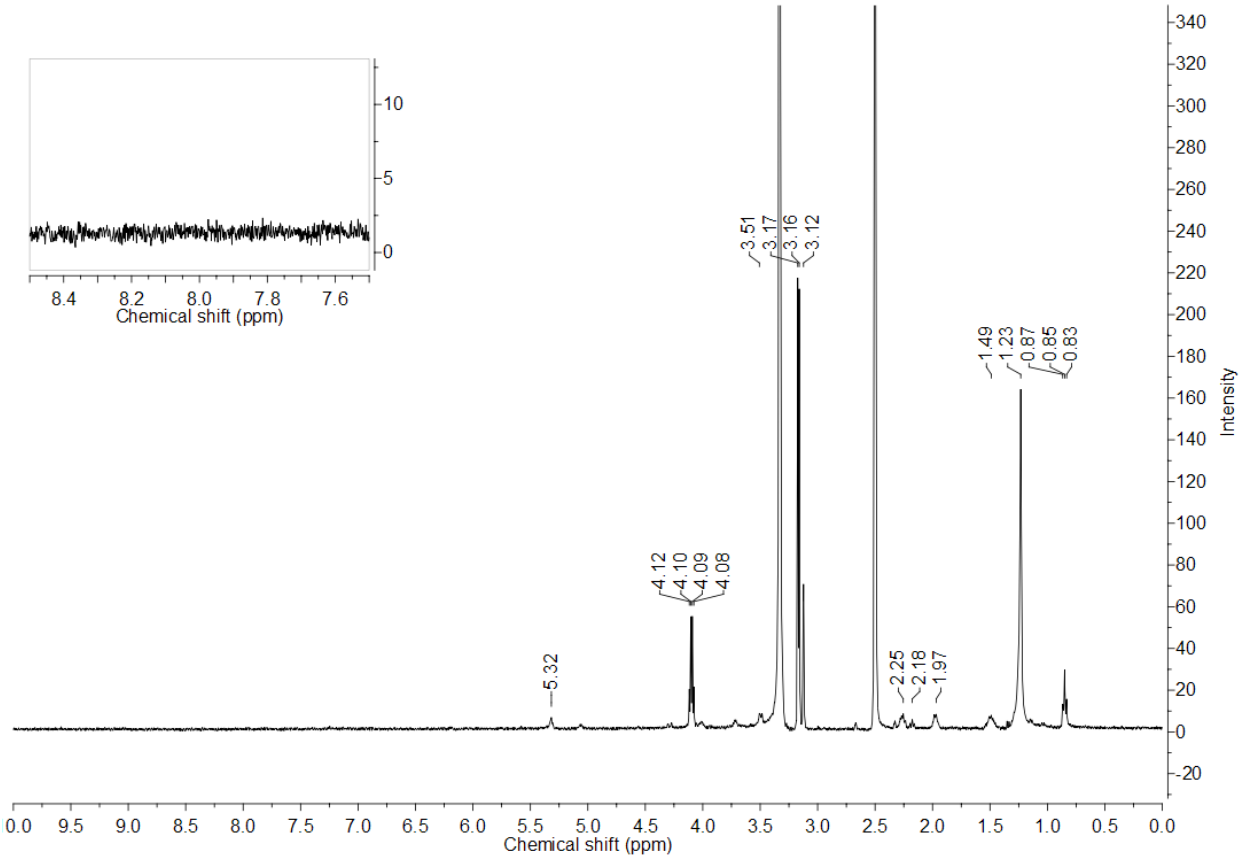

Figure S19 ^{1}H NMR analysis of the POPC control reaction. Full ^{1}H NMR spectrum of the butanol phase of only POPC control reaction that underwent five wet-dry cycles at 90°C. However, the peak corresponding to amide hydrogen that comes around 8 ppm, is absent in the spectrum (see inset). The solvent used was DMSO-d6.

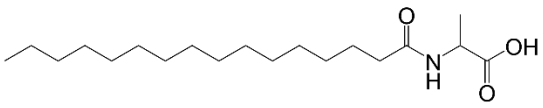

N-palmitoyl alanine (NPA)

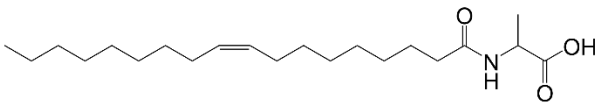

N-oleoyl alanine (NOA)

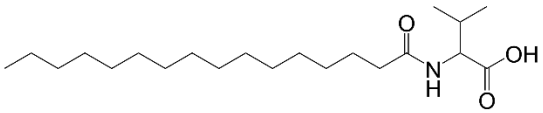

N-palmitoyl valine (NPV)

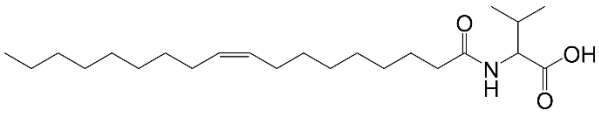

N-oleoyl valine (NOV)

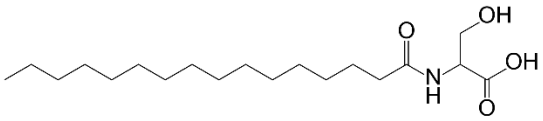

N-palmitoyl serine (NPS)

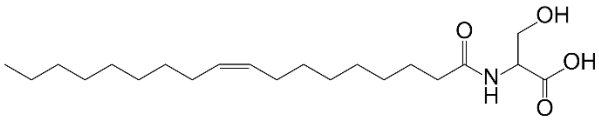

N-oleoyl serine (NOS)

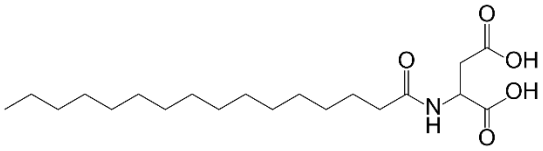

N-palmitoyl aspartic acid (NPD)

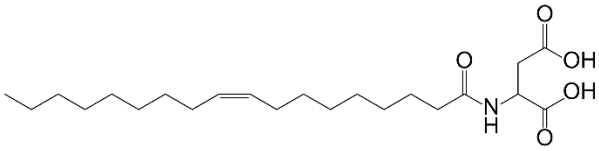

N-oleoyl aspartic acid (NOD)

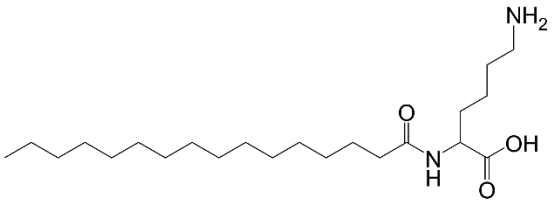

N-palmitoyl lysine (NPK)

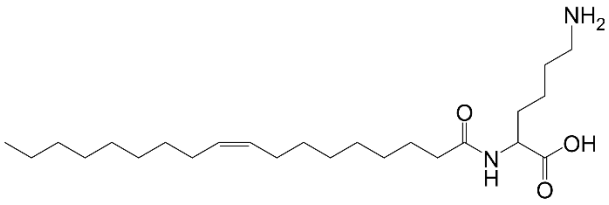

N-oleoyl lysine (NPK)

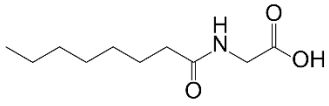

N-octanoyl glycine

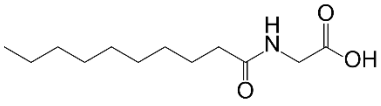

N-decanoyl glycine

Figure S20 The different kinds of NAAs formed in the amino acid and lipid variation experiments.

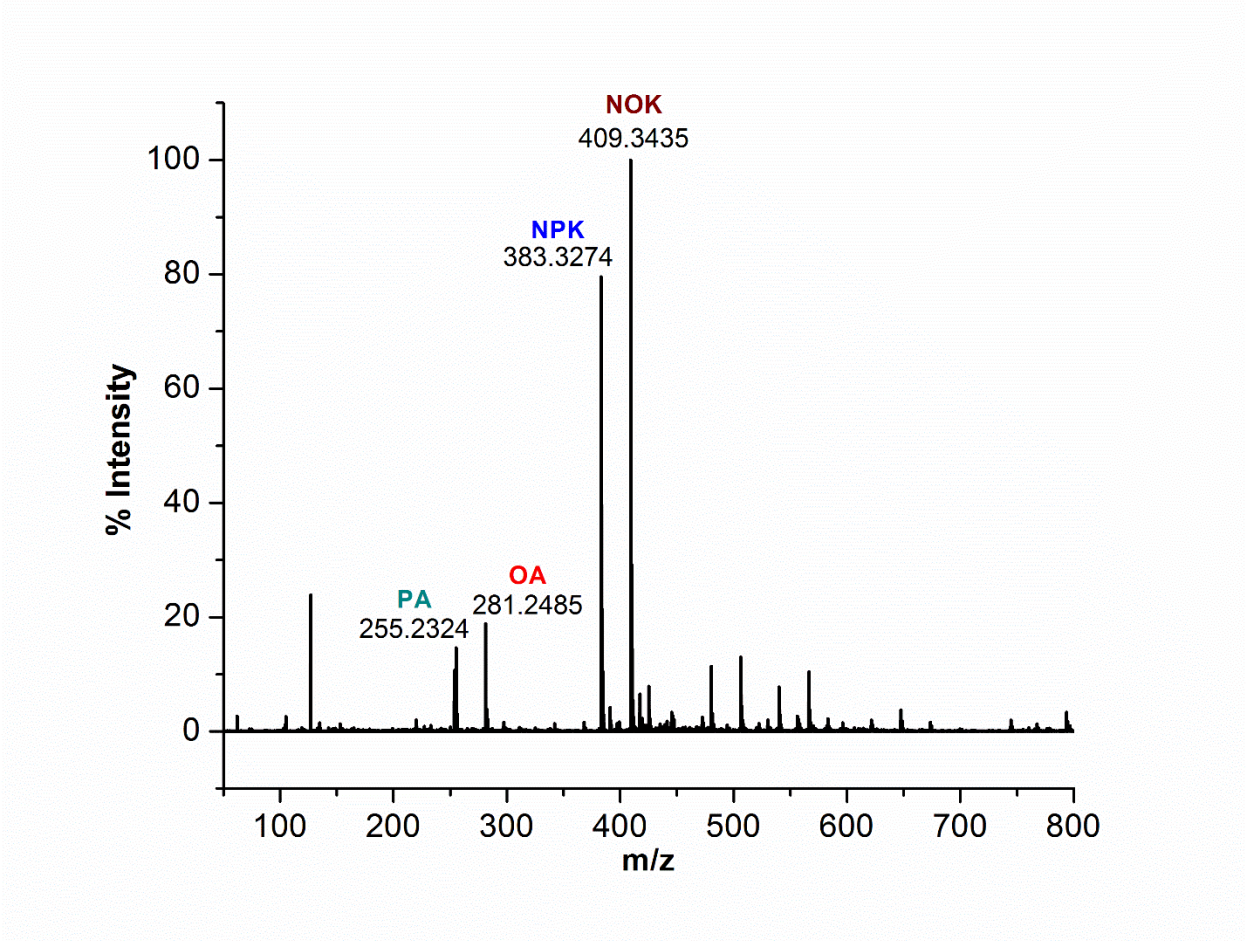

Figure S21 Formation of NAA in Lysine + POPC reaction. HRMS analysis of the butanol phase derived from the BH extraction of Lysine + POPC reaction shows predominant masses corresponding to N-palmitoyl lysine (NPK) and N-oleoyl lysine (NOK). Other masses corresponding to free fatty acids (PA and OA) are also observed potentially due to the hydrolysis of POPC. The analysis was performed in the negative ion mode.

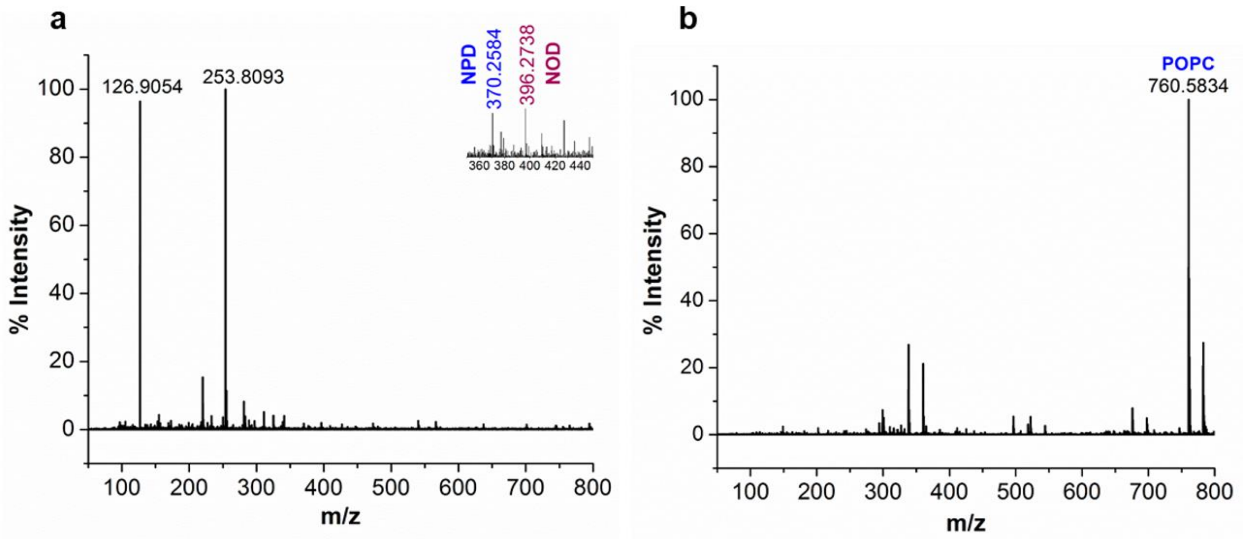

Figure S22 Formation of NAA in Aspartic acid + POPC reaction. HRMS analysis of the butanol phase derived from the BH extraction of Aspartic acid + POPC reaction in both (**a**) negative and (**b**) positive ion mode. Masses corresponding to N-palmitoyl aspartic acid (NPD) and N-oleoyl aspartic acid (NOD) are observed in **a** (see inset), although with less abundance, indicating the lower efficiency of aspartic acid towards NAA formation. This is also reflected in **b**, as most of the POPC in the reaction remained unreacted, which appears as a predominant mass in the positive ion mode. Peaks observed at 253 and 126 Da in **a** are solvent peaks.

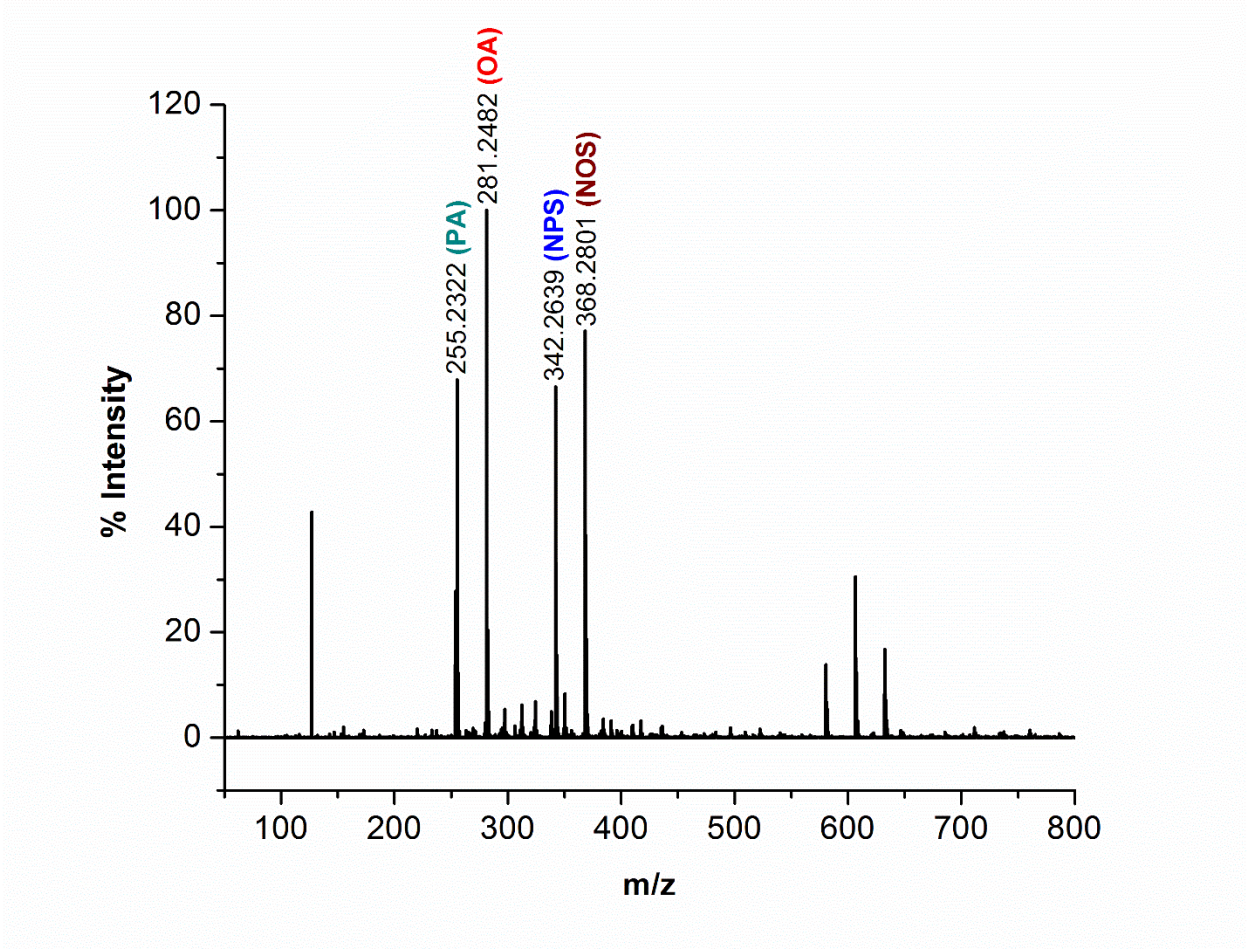

Figure S23 Formation of NAA in Serine + POPC reaction. HRMS analysis of butanol phase derived from the BH extraction of Lys + POPC reaction in the negative ion mode shows masses corresponding to N-palmitoyl serine (NPS) and N-oleoyl serine (NOS). Other masses corresponding to free fatty acids (PA and OA), potentially coming from the hydrolysis of POPC, are also observed with significant intensity.

Table S3 Different NAA masses observed during the HRMS analysis of the amino acid and lipid variation reactions.

NAA	Acronym	Exact mass	Theoretical mass	Observed mass	Error
			$[M-H]^-$	$[M-H]^-$	(ppm)
N-palmitoyl alanine	NPA	327.2773	326.2701	326.2692	-2.8
N-oleoyl alanine	NOA	353.293	352.2857	352.2845	-3.4
N-palmitoyl valine	NPV	355.3086	354.3014	354.3015	0.3
N-oleoyl valine	NOV	381.3243	380.317	380.3169	-0.3
N-palmitoyl lysine	NPK	384.3352	383.3279	383.3274	-1.3
N-oleoyl lysine	NOK	410.3508	409.3436	409.3435	-0.2
N-palmitoyl aspartic acid	NPD	371.2672	370.2599	370.2584	-4.1
N-oleoyl aspartic acid	NOD	397.2828	396.2755	396.2738	-4.3
N-palmitoyl serine	NPS	343.2723	342.265	342.2639	-3.2
N-oleoyl serine	NOS	369.2879	368.2806	368.2801	-1.4
N-decanoyl glycine	-	229.1678	228.1605	228.1599	-2.6
N-octanoyl glycine	-	201.1365	200.1292	200.1289	-1.5

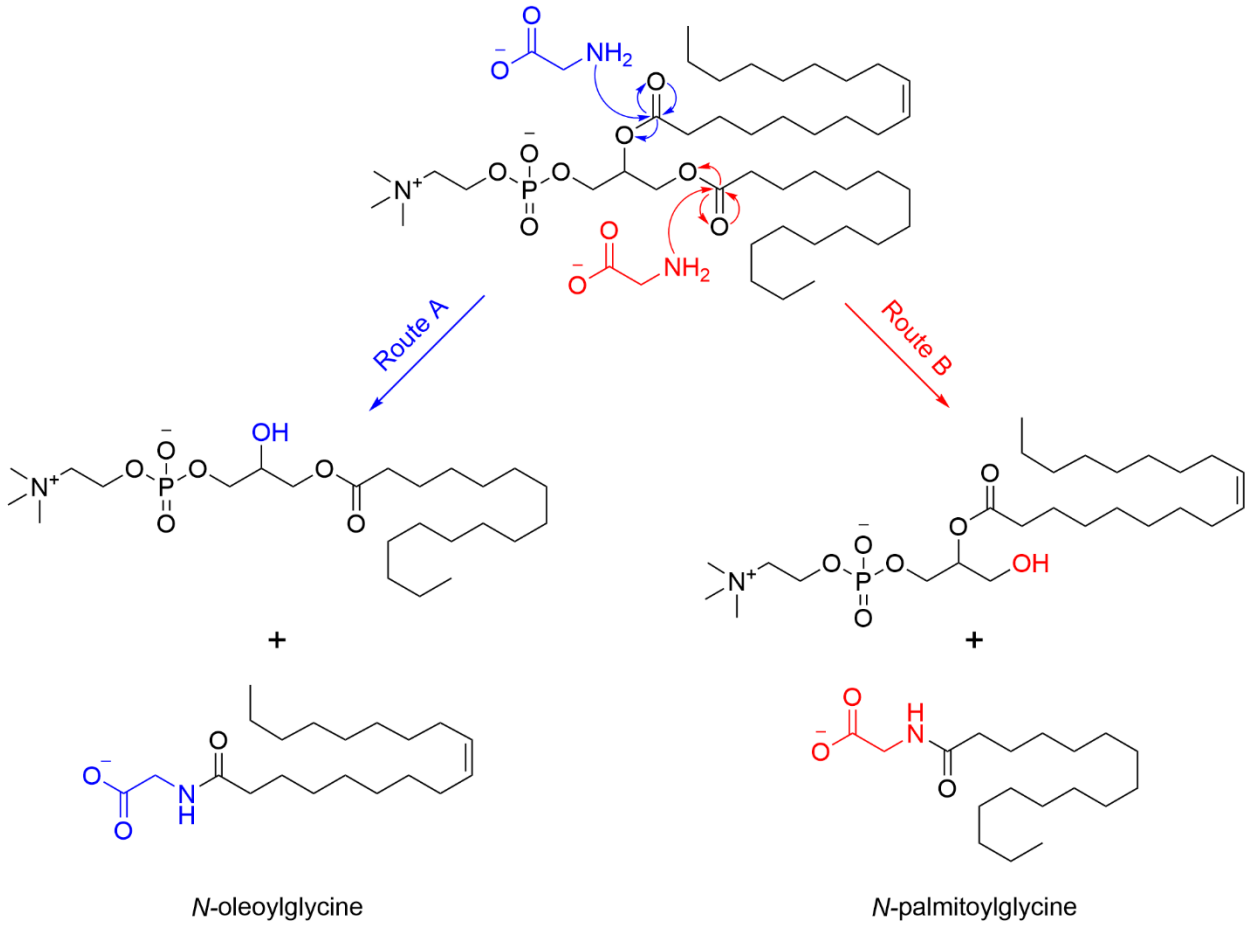

Figure S24 Reaction mechanism for the formation of NAAs in the Gly + POPC reaction. At alkaline pH, the deprotonated, nucleophilic amino group of Gly attacks the carbonyl carbon of one of the ester linkages of POPC, which forms corresponding NAA and POPC with one less acyl chain. If Gly attacks the ester linkage joining the oleoyl group to the glycerol backbone of POPC, then the resultant product will be N-oleoylglycine (Route A). Similarly, an attack on the ester bond linking palmitoyl group to the glycerol backbone of POPC will form N-palmitoylglycine (Route B).

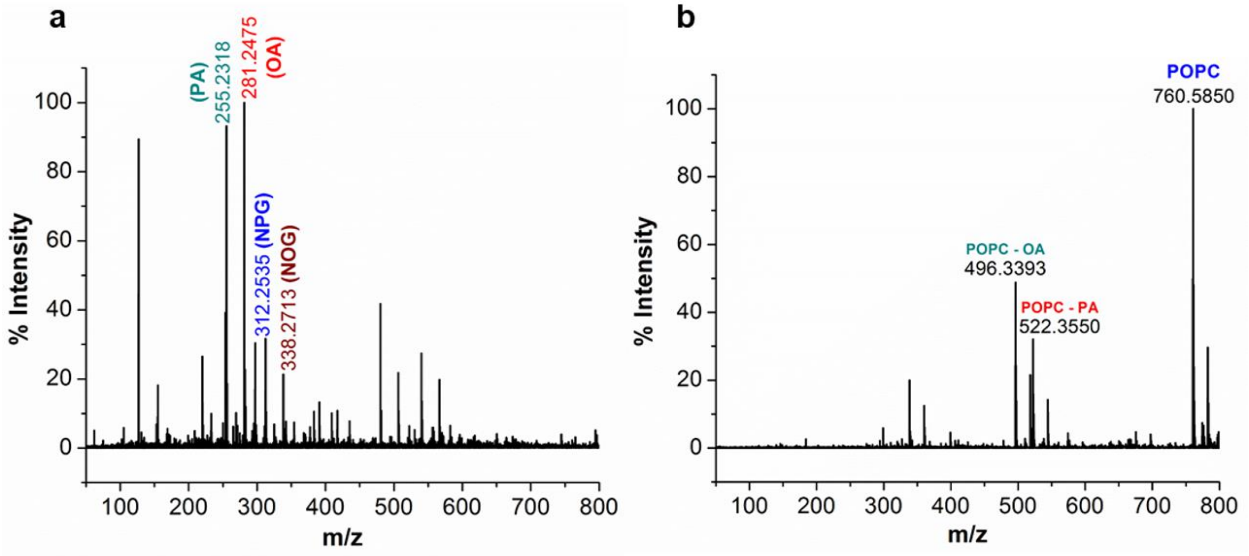

Figure S25 Formation of NAA in the Gly + POPC reaction at acidic pH. HRMS analysis of the butanol phase derived from the BH extraction of Gly + POPC reaction at pH 3 in both (**a**) negative and (**b**) positive ion mode. Masses corresponding to NPG and NOG are observed in **a**, although with lesser abundance, indicating the lower efficiency of NAA formation at acidic pH. This is also reflected in **b**, as most of the POPC in the reaction either remains unreacted or hydrolyzed to release free fatty acids (PA and OA), which are the predominant peaks in panel **a**.

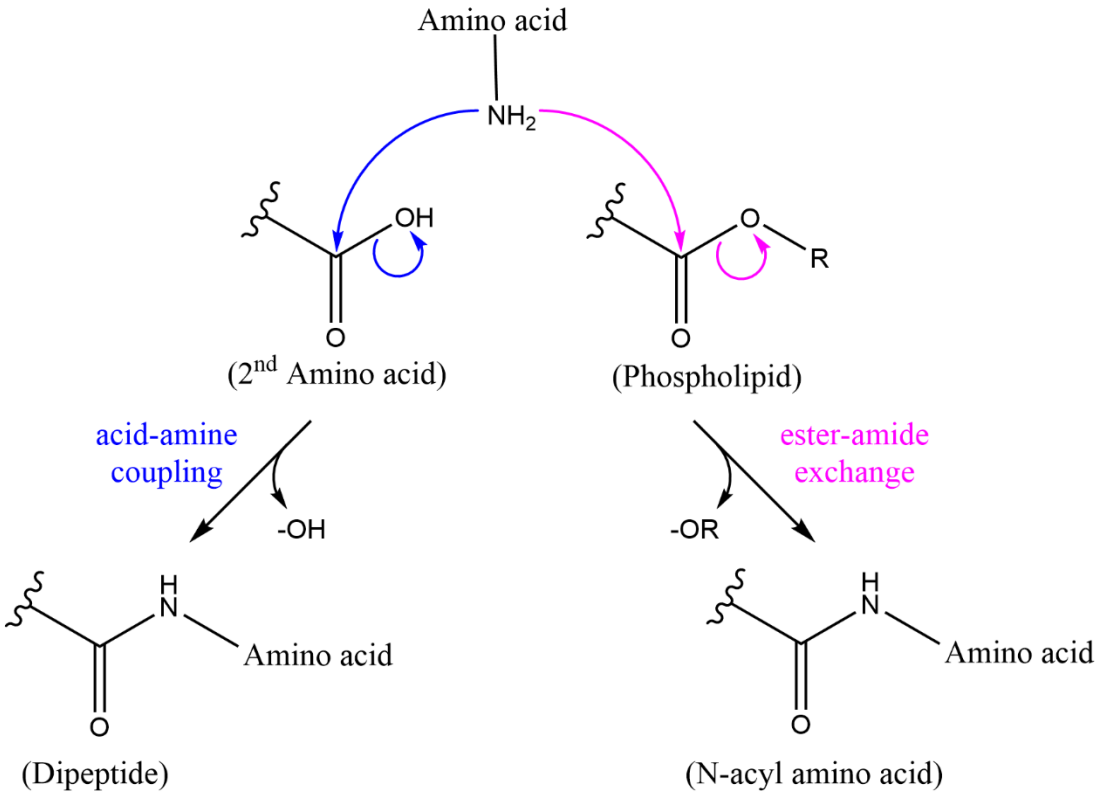

Figure S26 Mechanism of the amide bond formation in peptides versus in the NAAs. Two types of reactions that mainly occur in Gly + POPC reaction under wet-dry cycles are peptide synthesis and NAA synthesis, both of which involve the formation of an amide linkage, although via different modes. In peptide synthesis, the amide bond is formed via an acid-amine coupling that involves –OH as a leaving group. In the case of NAA synthesis, amide bond formation occurs through an ester-amide exchange reaction that involves –OR as a leaving group. The latter reaction would be kinetically more favorable than the first one, as –OR is a better leaving group than –OH.

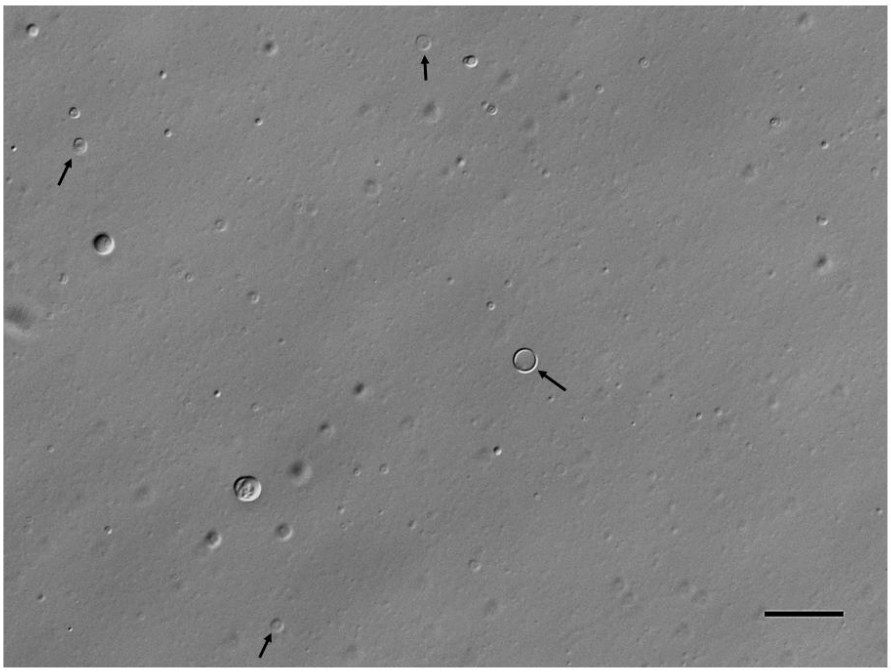

Figure S27 Formation of NOS vesicles at pH 3. N-oleoyl serine forms vesicles even at pH 3, which are indicated by black arrows in the figure. However, the efficiency of vesicle formation is lower as comparted to that at pH 4. Vesicles were observed under DIC microscopy. Scale bar is 20 µm.

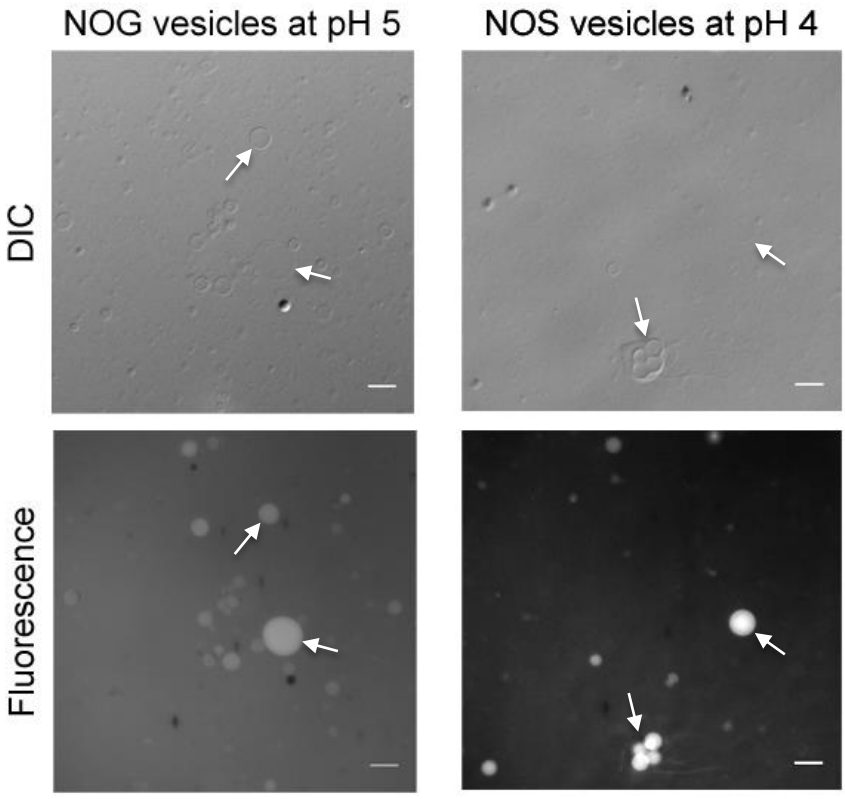

Figure S28 Encapsulation of calcein in NAA vesicles. Both NOG (left panel) and NOS (right panel) vesicles are able to encapsulate a fluorescent polar calcein molecule within them (indicated by white arrows), which confirms their vesicular nature. Vesicles were observed under both DIC and fluorescence microscopy. Calcein concentration used was 0.1 mM, which is below its self-quenching concentration. Scale bar is 10 µm.

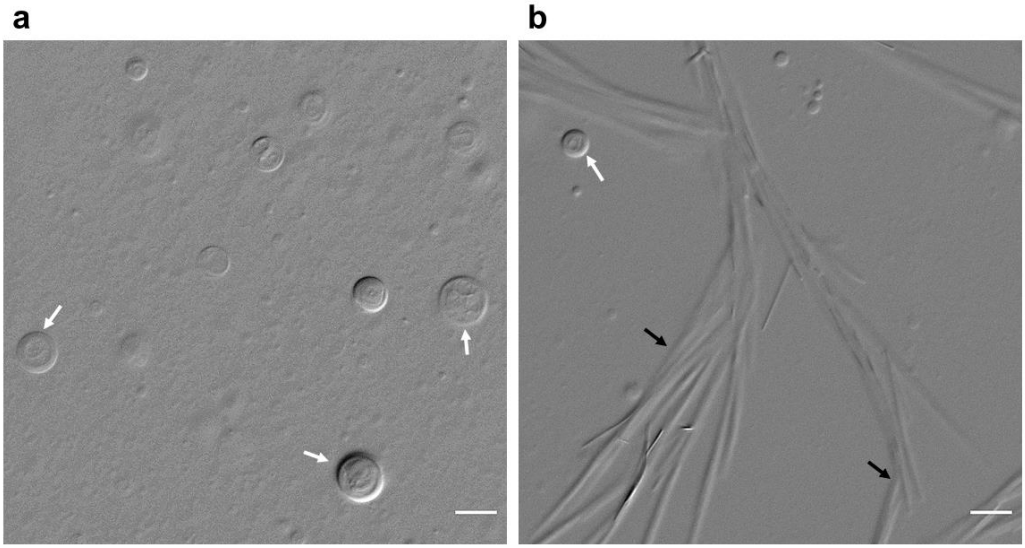

Figure S29 Temperature-dependent phase behavior of NOG. During vesicle preparation, 6 mM NOG pH 5 solution was incubated at 60°C for 1 hour and immediately subjected to microscopy. (**a**) Large number of vesicles (indicated by white arrows) were observed initially (0 min). (**b**) However, as the microscopy was performed at room temperature, this decrease in the solution temperature over the course of microscopy induced the conversion of the vesicles into fiber-like structures (indicated by black arrows) within a few minutes. Scale bar is 10 µm.

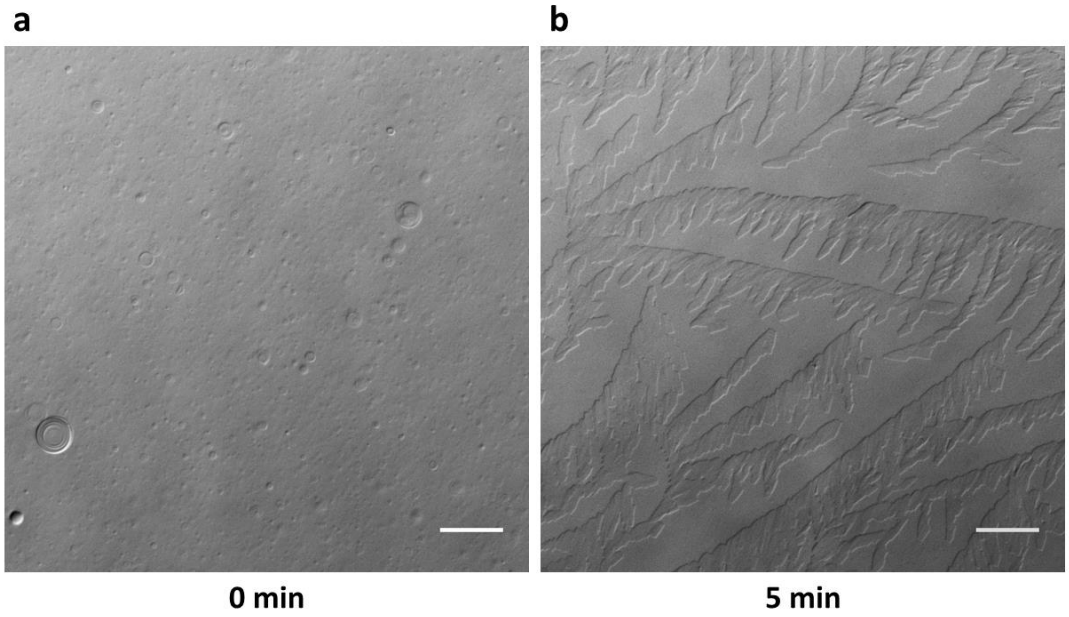

Figure S30 Temperature-dependent phase behavior of NOS. During vesicle preparation, 6 mM NOS pH 4 solution was incubated at 60°C for 1 hour and immediately subjected to microscopy. (**a**) Large number of vesicles were observed initially (0 min). (**b**) However, as the microscopy was performed at room temperature, this decrease in the solution temperature over the course of microscopy induced the conversion of the vesicles into crystalline structures within a few minutes. The morphology of these structures was different than that observed in the case of NOG (Fig S29). Scale bar is 20 µm.